# Critical Phenomena in the Gravitational Collapse of SU(2) Yang-Mills Fields

## A Numerical Study

by

Tyler Dodds

A THESIS SUBMITTED IN PARTIAL FULFILMENT OF
THE REQUIREMENTS FOR THE DEGREE OF

Bachelor of Science

(Physics)

The University Of British Columbia

April, 2007

# Abstract

We investigate the behaviour of abelian gauge, magnetic ansatz SU(2) Yang-Mills fields during gravitational collapse in spherical symmetry. The existence of critical phenomena is confirmed at the threshold of collapse. Two generic end states of evolution are found: flat space and black hole formation. The critical solution of a family of initial data separates the phase space into these end states. Type I critical phenomena, consisting of static critical solutions, minimum mass black hole formation, and scaling of solution lifetime near the critical solution, is the focus of this investigation. Finite difference approximations are used to solve the equations of motion of the system. These are formulated in two different manners. The first uses a first order in time approach. In this, auxiliary variables are defined so that their time derivatives are given by the equations of motion. Derivation of the funtamental variable from the auxiliary ones is required at each time interval in the simulation. This is the traditional formulation for solving problems numerically in general relativity. The second uses a second order in time approach. Here, no auxiliary variables are defined, and the equation of motion for the fundamental variable involves its second time derivative. Making the finite difference approximation is slightly more difficult, but derivation of the fundamental variable becomes unnecessary. Unpublished calculations seem to imply the breakdown of the first order in time method when applied to certain systems, and the second order method has been successfully utilized in the full-dimensional non-symmetric case [15]. These facts, along with the result that the second order method produces comparable results to the first order method in this study, indicates the possible use of the second order method in solving more general SU(2) systems. These generalizations would be obtained by removing the magnetic ansatz or the imposition of spherical symmetry.

# Table of Contents

# List of Figures

# List of Tables

# Acknowledgements

I would like to thank my supervisor, Matthew Choptuik, for his invaluable guidance, help and support during my studies of numerical relativity.

# Chapter 1

# Introduction

In general relativity, as in all areas of physics, most problems are simply too intractable to be solved in closed form. When faced with this problem, there are two general directions to head in. The first direction is to make some clever approximation so as to yield a solvable problem. This has the advantage of yielding a general closed form solution, making it easier to see the dependence of the solution on the problem's parameters. Often, this can give great insight into the structure of the problem and its solution. However, the solution is only approximate, and one needs to fully understand how much of the solution's behaviour the approximation truly describes. The second direction is to attempt to solve the full problem exactly with some sort of numerical method. The disadvantage here is that parameters must be explicitly given beforehand, and thus many different solutions will be required to discern the dependence of the problem on its parameters. The advantage is that the solution is as exact as the numerical method and computational resources will allow. The solutions truly are simulations, in that they behave exactly as the theoretical system would, and can give us a very good picture of the physics described by the theory.

Numerical relativity is the result of heading in this second direction in an attempt to get a detailed picture of how systems behave under gravity as described by the theory of general relativity. One of the many interesting results obtained from having these full simulations is the existence of *critical phenomena*, the behaviour associated with a system on the verge of collapse to a black hole.

## 1.1 Critical Phenomena

A generic, isolated system acting under general relativity evolves on a long time scale based on the competition between the dispersive effects of the kinetic energy of the system and its gravitational self-attraction, or the explicit self-interaction of the matter. With minimal gravitational interaction, a system with sufficient kinetic energy will tend to disperse to infinity. Systems with strong gravitational self-interaction will tend to collapse, forming

a black hole. A binary system of two black holes orbiting each other, for example, will also collapse into a single black hole, due to emission of gravitational waves [13].

Critical phenomena occur when the gravitational self-interaction becomes just strong enough to form a black hole. Since the initial data uniquely determines the evolution of the system, it can be used to control the end state of evolution of the system. In this sense, the parameters of the initial data do more than just specify the starting point of the system: they also distinguish between the two generic end states of a system, flat space (after dispersal to infinity) and black holes. These parameters thus form a basis for a phase space of the system, where the term *phase* here means the state of the system after a sufficiently long time.

To be more precise, we choose the parameters of the initial data, $p_i$, so that they show this kind of control over the end state of the system. Fixing all parameters $p_i$ except for a particular $p_j$ corresponds to a (single parameter) family of initial data governed by the parameter $p_j$, as it is varied. In general it is fairly easy to choose parameters that scale with the gravitational self-interaction of the system, and specifically that result in the following properties:

- Sufficiently small values of $p$ lead to dispersal of the system to infinity for sufficiently long times, leaving behind flat space.
- Sufficiently large values of $p$ lead to gravitational collapse of the system and the eventual formation of a black hole.
- There exists a *critical value* of the parameter, $p^*$, that separates the two end states of evolution. Flat space results for $p < p^*$, while a black hole is formed for $p > p^*$.

The *critical solution* for this family of initial data is the solution when $p = p^*$. We call initial data with $p < p^*$ *subcritical*, and initial data with $p > p^*$ *supercritical*. One could equally well define $p$ in the opposite manner, where black holes are formed for $p < p^*$. It is important to note that this family, and hence $p^*$, depend on the values of the other fixed parameters.

The system wherein critical phenomena were first discovered was the massless scalar field, minimally coupled to gravity, in spherical symmetry. The advantage of the scalar field model is that it propagates at the speed of light, effectively mimicking gravitational radiation. Unlike gravitational radiation, however, it exists in spherical symmetry and is a simple enough problem to allow for accurate calculations that can properly resolve the

critical behaviour. See Gundlach's review article for an excellent history of the study of gravitational critical phenomena [11].

Systems display many interesting types of behaviour at and around their critical solutions. There are two broad clases of critical phenomena, named types I and II in analogy to first and second order phase transitions, since the critical behaviour is also analogous to that seen in such phase transitions. Like phase transitions, each type of critical phenomenon shows different behaviour in detail. However, both types share the *universality* of the critical solution. This means that the critical solution is unique, up to rescaling of units, across different families of initial data. Figure 1.1 shows the universality of a near-critical solution with a massless scalar field as the matter source. Each of the four solutions evolves with identical profiles over time, despite being generated from different families of initial data.

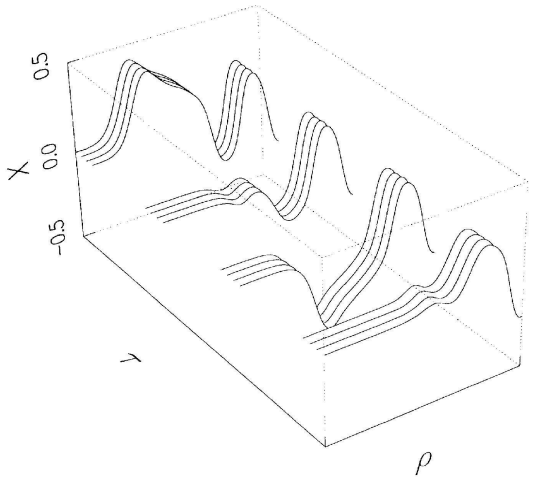


Figure 1.1: Universality of a near-critical solution of a massless scalar field. At each time coordinate $\tau$ is a group of four different solutions of a massless scalar field. Each profile has a different family of initial data, with scaling chosen for each family to maximize agreement at the earliest $\tau$. The consistent evolution shows the universality of the critical solution, independent of its initial form. Figure taken from [5].

Both types of critical phenomena can be understood in terms of the phase space, where the so-called critical hypersurfaces separate the regions of different final states of the system. A system beginning on a critical hypersurface never leaves it. In this view, the critical solution is an attracting

equilibrium point within this critical hypersurface. Associated with the solution are an infinite number of stable, decaying modes tangential to the hypersurface and a single unstable, growing mode that is not tangent [11]. This unstable mode will eventually control the dynamics, taking solutions away from the critical hypersurface towards one of the generic system end states. In tuning towards the critical solution, we are essentially tuning out this single unstable mode.

### 1.1.1 Type II Critical Phenomena

Type II critical phenomena were the first discovered, with the choice of a single massless scalar field as the matter source [5]. It is characterized by the presence of black holes of arbitrarily small mass, and a continuous transition from the flat-space regime to the black hole regime.

The first feature of type II critical behaviour is the scaling of the black hole mass with the parameter $p$. In the region $p > p^*$, where black holes form, it is found that the mass of the black hole, $M_{\mathrm{BH}}$, varies as

$$M_{\mathrm{BH}} = c_f |p - p^*|^{\gamma}. \tag{1.1}$$

Here, $\gamma \sim 0.37$ is a family-independent dimensionless parameter; only the scaling factor $c_f$ depends on the family of initial data. Figure 1.2 shows the mass scaling relationship in type II black hole formation for a massless scalar field. The identical slopes seen for all three types of initial data indicate the same power law growth of the black hole mass with parameter $p$, regardless of the form of the initial data.

This is what gives rise to "infinitesimal" mass black holes, as $p \to p^*$. In effect this is a continuous transition in parameter space, viewing the black hole mass $M$ as the parameter of interest of the end state of evolution. The transition from the $M = 0$ region of parameter space (flat space) to the $M > 0$ (black hole) region is continuous as $p$ varies across $p^*$. This is analogous to the definition of second order phase transitions, and is similarly at the heart of the interesting behaviour near the critical solution.

The second interesting feature of type II critical behaviour is called *scale echoing*. The critical solution $\phi_{\mathrm{crit}}(r, t)$ is invariant under a certain scaling of both space and time, namely

$$\phi_{\mathrm{crit}}(r, t - t^*) = \phi_{\mathrm{crit}}(e^{\Delta} r, e^{\Delta}(t - t^*)), \tag{1.2}$$

for $t < t^*$, with $t^*$ being the time after which all scaling invariance has finished. Here $\Delta \sim 3.44$ is a dimensionless parameter that is, like the critical

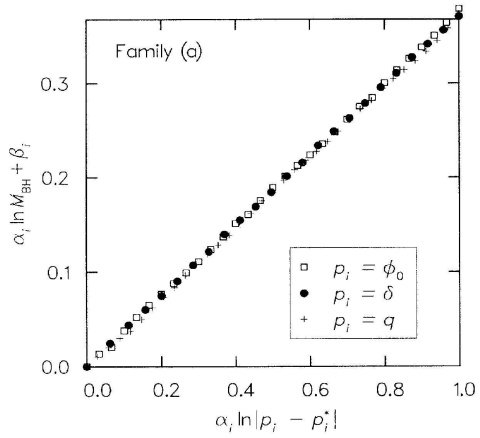


Figure 1.2: Black hole mass scaling in type II gravitational collapse of a massless scalar field. The black hole mass variation with the difference of the initial data parameter $p$ from the critical value $p^*$ is plotted on a log-log scale. Each of the three markers corresponds to a different type of initial data. Each family of markers is plotted so as to normalize the domain and place the smallest-mass black hole at the origin. Figure taken from [5].

solution, family-independent. Figure 1.3 shows this behaviour for a near-critical solution of a massless scalar field, where the profile is identical to one at a time $e^{\Delta}$ closer to $t^*$, but on a spatial scale $e^{\Delta}$ smaller.

### 1.1.2 Type I Critical Phenomena

There is also a classification of type I critical behaviour, which is the focus of this investigation. It is characterized by the creation of a minimum mass black hole for parameter values just above the critical value $p^*$. Here the black hole mass $M$ varies discontinuously as $p$ crosses $p^*$, from the $M = 0$ flat space region for $p < p^*$ to the $M \geq M_0$ region for $p > p^*$, with $M_0$ the minimum black hole mass. This is analogous to the discontinuous nature of first order phase transitions, where system variables change abruptly upon phase change.

What one finds in type I critical phenomena is that the critical solution acts as an unstable equilibrium point in phase space. Solutions that are either slightly supercritical or subcritical will begin collapse, but stop at the critical solution for a certain length of time before dispersing to infinity or completely collapsing. The closer $p$ approaches $p^*$, the longer is the *lifetime*

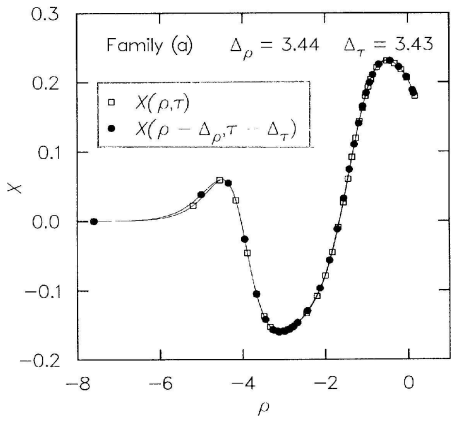


Figure 1.3: Scale echoing property of a near-critical solution of a massless scalar field. The curve marked with solid circles is on a spatial scale $e^{\Delta_\rho} \approx 30$ times smaller than the curve marked by open squares, but is at a time $e^{\Delta_\tau} \cong e^{\Delta_\rho}$ closer to the time when the 'echoing' behaviour ceases. The two profiles agree under this specific scaling. Figure taken from [5].

of this unstable solution. In fact, we get a scaling law similar to the mass scaling in type II critical phenomena. The lifetime, $\tau$, scales as

$$\tau = d_f - \sigma \ln |p - p^*|. \tag{1.3}$$

As with the scaling exponent in the type II case, $\sigma$ is independent of the family of initial data. Only the constant $d_f$ depends on the particular family.

Type I critical solutions do not exhibit the same type of scale invariance that type II solutions do. Instead, they exhibit invariance under purely temporal translations. If they are invariant under certain discrete translations, the critical solutions are seen to be time-periodic. If they are invariant under continuous time translations, as will be the case in this work, the critical solutions are static. These static critical solutions satisfy the equations of motion and are full static solutions for the matter choice.

## 1.2 Yang-Mills Fields

Gravitational critical phenomena are not peculiar to a certain few types of matter. Indeed, critical phenomena of some sort have been found in all matter types investigated to date [11]. Among the matter types investigated are massive scalar fields, scalar fields coupled to electromagnetism, perfect

fluids, and Yang-Mills fields, all of which generate critical behaviour. The few investigations in axial symmetry suggest that critical behaviour occurs in more general contextxs than spherical symmetry [1, 8].

In this investigation we focus on the critical behaviour of Yang-Mills fields – in particular, an SU(2) field in spherical symmetry restricted to the purely magnetic sector of the theory, and with the so-called abelian gauge. This will henceforth be referred to as an abelian gauge magnetic ansatz SU(2) field. This follows the work of Choptuik, Chmaz and Bizon [7]. A description of the SU(2) Yang-Mills field, restriction to spherical symmetry, and implementation of the magnetic ansatz and choice of abelian gauge can be found in [9]. The Yang-Mills fields are perhaps the most well-known examples of gauge theories, which are predicated on being able to perform symmetry transformation locally, rather than being restricted to global application. Interest in Yang-Mills fields arose as a result of an attempt to understand the nature of fundamental interactions from a quantum field-theoretical perspective. This was quite a successful attempt: the SU(3) field describes quantum chromodynamics, while the SU(2) field is integral in understanding the electroweak force [12].

Under the restrictions imposed for this investigation, the Yang-Mills field is to be viewed as a simple model that can be used to explore the possible dynamics and phenomena that can arise in the collapse of a non-abelian gauge field. As this work is classical, in the gravitational (rather than quantum) regime, we do not expect the Yang-Mills field to be a model for a particular phenomenon or system. However, this work can give an indication of the behaviour of these gauge theories coupled to gravity, without requiring a unified quantum gravitational theory.

## 1.3 Finite Difference Approximations

In this work, we consider the type I critical behaviour of the abelian gauge, magnetic ansatz SU(2) field in spherical symmetry. The aim is to solve the equations of motion of this field, as well as the equations determining the general relativistic gravitational field, using finite difference approximations. Such approximations use a grid on the spacetime domain and approximate derivatives, equations of motion, and solutions on this grid.

Traditionally, numerical studies of general relativity cast the relevant equations in a first order in time manner. With this approach, an equation with multiple time derivatives is split up into multiple equations with fewer

time derivatives. For instance, the wave equation

$$\phi_{tt} = \phi_{rr} \tag{1.4}$$

is naturally a single second order in time (with two time derivatives) equation. We use the notation of $\phi_x \equiv \partial\phi/\partial x$ for partial differentiation. However, with the definitions $\Phi \equiv \phi_r$ and $\Pi \equiv \phi_t$, we get

$$\Pi_t = \Phi_r \tag{1.5}$$

$$\Phi_t = \Pi_r. \tag{1.6}$$

The equation describing the time evolution of $\Pi$, (1.5), follows from the initial equation, while that for the time evolution of $\Phi$, (1.6), follows from the commutation of partial differentiation.

First order in time schemes use auxiliary variables such as $\Phi$ and $\Pi$. They are defined so that the set of equations reduces as much as possible to equations yielding single time derivatives of one of these auxuilaury variables. Often these definitions help to simplify the equations even further. This might be accomplished by replacing other spatial or temporal derivatives of fundamental variables with auxiliary variables or their derivatives. It is often more straightforward to write a finite difference approximation for a system containing only single derivatives than one with second (or higher) derivatives.

The advantages of this first order formulation are numerous. However, while the introduction of these auxiliary variables can greatly simplify the equations, this gives the auxiliary variables precedence over the fundamental variables they are replacing. In the case of the wave equation, only derivatives of the function $\phi$ appear in the equation (and also most boundary conditions), so subsidiary calculation of $\phi$ from its derivative $\Phi$ is straightforward and furthermore is unnecessary in solving the equation. In other cases (such as for the set of equations considered in this investigation) the auxiliary variables can replace the fundamental variable's derivatives, but not the variable itself. In this case the fundamental variable of interest, such as $\phi$ above, becomes a derived quantity of the problem, rather than a quantity calculated directly by the new system of equations. Calculation of the fundamental variable is necessary throughout the simulation — a process which introduces more error. We will refer to this calculation as the 'derivation' of the fundamental variables from the auxiliary variables to emphasize that, in this work, this is a process involving the non-trivial integration of an auxiliary variable.

Second order in time methods (for equations with second time derivatives) solve directly for the fundamental variable of interest. Second derivatives are approximated directly. In cases where they are the highest order derivatives, no auxiliary variables are required. The aim is to be able to sidestep any unwanted behaviour introduced by the derivation error. This investigation will be looking at the critical phenomena of the chosen SU(2) Yang-Mills field using both a first order and second order numerical formulation. Its goal is to investigate the strengths and weakness of the second order method in comparison to the first order one, using the spherically symmetric SU(2) case as a simpler test case to determine if second order methods could be employed to investigate the behaviour of a general SU(2) Yang-Mills field. In this case the relevant system of equations would have more fundamental variables and would fully incorporate all spatial dimensions. Indeed, unpublished calculations seem to imply the breakdown of the first order in time method when applied to certain systems, and the second order method has been successfully utilized in the full-dimensional non-symmetric case [15]. This work looks to replicate that success in the context of studying SU(2) Yang-Mills fields, looking first at a simplified version of the problem.

## 1.4 Outline

In Chapter 2 we begin with a brief overview of the relevant theory of the problem. The focus is on the equations that describe the time evolution of the Yang-Mills field and the geometry of the spacetime.

Chapter 3 delves deeply into the theory of finite difference approximations. When building a numerical simulation, it is very important to be able to introduce the proper finite difference approximations and to understand the solution error and convergence properties that result.

Chapter 4 describes the critical phenomena found in SU(2) Yang-Mills fields. It contains checks that the simulations are converging and behaving as expected. The first order and second order formulations are compared here.

Chapter 5 discusses the critical phenomena found and explores the potential for the use of second order methods in other numerical simulations of generalized versions of the SU(2) fields considered in this work.

# Chapter 2

# Theory

## 2.1 3+1 Formalism of General Relativity

Most numerical work in relativity decomposes the spacetime into the temporal dimension and spatial dimensions. The most frequently used formalisms derive from the 3+1 (ADM) formalism, first formulated by Arnowitt, Deser and Misner [2]. This views the spacetime as a family of three-dimensional spacelike hypersurfaces. Since ordinary matter moves along timelike curves, its trajectory will be given by a unique position along each hypersurface. This formalism will generate the spacetime and matter field as an initial value problem, once a particular initial hypersurface is completely characterized.

## 2.2 Coordinates and Spherical Symmetry

In all the work that follows, we work in "geometrized" units where the speed of light $c = 1$ and the gravitational constant $G = 1$. Then all units are measured as a power of a certain fundamental unit; in relativity, this is often taken as the cm. Time, for example, would be measured in cm, with the speed of light $c$ being the conversion factor between the more usual units of s.

In relativity, the metric provides infinitesimal distances between neighbouring points in spacetime, thus describing its geometry. The most general time-dependent metric under spherical symmetry can be written [14] as

$$ds^2 = (-\alpha^2 + a^2\beta^2)dt^2 + 2a^2\beta dt dr + a^2 dr^2 + r^2 b^2 d\Omega^2, \tag{2.1}$$

with $\alpha$, $\beta$, $a$ and $b$ functions of $r$ and $t$, and

$$d\Omega^2 = d\theta^2 + \sin^2\theta d\varphi^2, \tag{2.2}$$

which is the metric on the unit 2-sphere. Here, $\theta$ and $\varphi$ comprise the usual azimuthal and polar angles in spherical coordinates. It is convenient to

adopt so-called polar and areal coordinates, defined by $\beta = 0$ and $b = 1$ [3]. This simplifies the metric to

$$ds^2 = -\alpha^2 dt^2 + a^2 dr^2 + r^2 d\Omega^2. \tag{2.3}$$

This makes constant-$r$ trajectories normal to the spacelike hypersurfaces. Furthermore, the coordinate $r$ provides a measure of the proper surface area in this case, with $A = 4\pi r^2$.

These coordinates in spherical symmetry make it convenient to define the mass aspect function by

$$a^2(r,t) = \left(1 - \frac{2m(r,t)}{r}\right)^{-1}. \tag{2.4}$$

Then $m(r,t)$ is the gravitating mass inside a radius $r$ at time $t$. In spherical symmetry, $2m/r_B = 1$ at the radius of a black hole, $r_B$. By monitoring the quantity $2m/r_B$, we can determine when black hole formation is imminent, as $2m/r_B$ approaches 1.

## 2.3 Yang-Mills Fields in Spherical Symmetry

Under the imposition of spherical symmetry, the choice of metric (2.3), and the particular assumptions regarding the SU(2) field (namely, abelian gauge and magnetic ansatz), it happens that one can view the matter content as a single function $W(r,t)$, which acts analogously to a scalar field with a self-interacting potential [7]. There is an associated Lagrangian scalar

$$L_M = -\left(\frac{g^{\mu\nu}\nabla_\mu W \nabla_\nu W}{r^2} + \frac{1}{2}\frac{(1-W^2)^2}{r^4}\right). \tag{2.5}$$

Then, by the principle of minimal coupling, one can picture the system as being given by a total Lagrangian which is the sum of the free gravitational Lagrangian $\mathcal{L}_g$ and the matter Lagrangian $\mathcal{L}_M$,

$$\mathscr{L} = \mathcal{L}_g + \mathcal{L}_M = \sqrt{-g}\,(R + L_M)\,, \tag{2.6}$$

with $R$ the Ricci scalar, and $g$ the determinant of the metric (2.3).

One physically important quantity is the energy density,

$$\rho = \frac{1}{4\pi a^2 r^2}\left(W_r^2 + \frac{a^2}{\alpha^2}W_t^2 + \frac{a^2}{2r^2}(1-W^2)^2\right), \tag{2.7}$$

which will be used to determine conditions on $W$ and $a$ at $r = 0$ [9].

## 2.4 Equations of Motion for Yang-Mills Fields

The equations giving $a$ and $\alpha$ come from the general 3+1 formalism in spherical symmetry, with the specific choice of coordinates used here. The equation of motion for $W$ is given by the variational principle, using the effective Lagrangian (2.6) [6].

Solution of the equations of motion for the system given by the Lagrangian (2.6) can be reduced to solving a system of partial differential equations for the metric coefficients and the derivatives of the Yang-Mills potential:

$$\Phi_t = \left(\frac{\alpha}{a}\Pi\right)_r \tag{2.8}$$

$$\Pi_t = \left(\frac{\alpha}{a}\Phi\right)_r + \frac{a\alpha}{r^2}W(1-W^2) \tag{2.9}$$

$$\begin{aligned} & \frac{a_r}{a} + \frac{a^2-1}{r^2} \\ -\frac{1}{r}\left(\Phi^2 + \Pi^2 + \frac{a^2}{2r^2}(1-W^2)^2\right) &= 0 \end{aligned} \tag{2.10}$$

$$\begin{aligned} & \frac{\alpha_r}{\alpha} - \frac{a^2-1}{r^2} \\ -\frac{1}{r}\left(\Phi^2 + \Pi^2 - \frac{a^2}{2r^2}(1-W^2)^2\right) &= 0, \end{aligned} \tag{2.11}$$

where

$$\Phi = W_r \tag{2.12}$$

$$\Pi = \frac{a}{\alpha}W_t, \tag{2.13}$$

so that

$$W(r,t) = W_0 + \int_0^r \Phi(x,t)dx \tag{2.14}$$

describes the Yang-Mills field. These equations are the set of first order in time (or simply first order) equations because the variables $\Phi$ and $\Pi$ are evolved in time by PDEs containing only a single time derivative.

The definitions of $\Phi$ and $\Pi$ can be substituted into the first order equations to yield the second order in time equations:

$$\left(\frac{a}{\alpha}W_t\right)_t = \left(\frac{\alpha}{a}W_r\right)_r + \frac{a\alpha}{r^2}W(1-W^2) \tag{2.15}$$

$$\frac{a_r}{a} + \frac{a^2-1}{r^2} \tag{2.16}$$
$$-\frac{1}{r}\left(W_r^2 + \frac{a^2}{\alpha^2}W_t^2 + \frac{a^2}{2r^2}(1-W^2)^2\right) = 0$$

$$\frac{\alpha_r}{\alpha} - \frac{a^2-1}{r^2} \tag{2.17}$$
$$-\frac{1}{r}\left(W_r^2 + \frac{a^2}{\alpha^2}W_t^2 - \frac{a^2}{2r^2}(1-W^2)^2\right) = 0.$$

Equation (2.15) gives the second order in time (second time derivative) equation for $W$.

## 2.5 Regularity, Initial and Boundary Conditions

### 2.5.1 Regularity Conditions

When $r = 0$, we are at one edge of our numerical domain. This is not a physical boundary but merely the center of the spherically symmetric system. Regularity conditions simply demand that the system behaves normally at the origin, namely that quantities such as the energy density are all finite. Looking at the energy density $\rho$, given in (2.7), as $r \to 0$, we place certain restrictions on $W$ in order to keep $\rho$ finite. In particular the term

$$\frac{1}{8\pi}\left(\frac{1-W^2}{r^2}\right)^2 \tag{2.18}$$

needs to remain finite as $r \to 0$, so we have that

$$1 - W^2 = O(r^2) \quad \text{as} \quad r \to 0. \tag{2.19}$$

Then for small $r$, we expand $W$ as

$$W(r,t) = W_0(t) + W_1(t)r + W_2(t)r^2 + O(r^3), \tag{2.20}$$

so that

$$W^2(r,t) = W_0(t)^2 + 2W_0W_1r + (2W_0W_2 + W_1^2)r^3 + O(r^3). \tag{2.21}$$

Thus we immediately see from (2.19) that

$$W_0(t) = \pm 1 \qquad\qquad W_1(t) = 0 \tag{2.22}$$

and hence

$$W(r,t) = \pm 1 + O(r^2) \qquad W_t(r,t) = O(r^2) \qquad W_r(r,t) = O(r). \tag{2.23}$$

Continuity in time requires that $W(0,t)$ stays constant, and without loss of generality we can choose the + sign, since the equations of motion (2.15) – (2.17) are symmetric under the transformation $W \to -W$. Hence, the regularity conditions for $W$ are the origin are

$$W(0,t) = 1 \qquad W_t(0,t) = 0 \qquad W_r(0,t) = 0. \tag{2.24}$$

As the origin is not a special point, we require spacetime to be locally flat there, the same as all other non-singular points. So as $r \to 0$, we require the metric (2.3) to approach the flat space metric in spherical coordinates,

$$ds^2 = -dt^2 + dr^2 + r^2 d\Omega^2. \tag{2.25}$$

This implies that $a(0,t) = 1$, otherwise a conical singularity develops at the origin. In other words, the ratio of proper circumference of a circle to its proper radius does not approach $2\pi$ as $r \to 0$. To see this, a circle around the origin is parametrized by $\phi$ if $\theta = \pi/2$, and the proper circumference is

$$\int_0^{2\pi} r \sin(\pi/2) d\phi = 2\pi r. \tag{2.26}$$

The proper radius, however, is

$$\int_0^r \left( a(0,t) + \tilde{r} a'(0,t) + O(\tilde{r}^2) \right) d\tilde{r} = a(0,t) r + O(r^2). \tag{2.27}$$

Now, as $r \to 0$, their ratio approaches $2\pi/a(0,t)$, which is not the locally flat value of $2\pi$ unless $a(0,t) = 1$.

### 2.5.2 Initial Conditions

Since we want to consider the critical phenomena occuring as a result of gravitational collapse, we want to set up the Yang-Mills field so that it is initially collapsing. Since we are in principle able to choose any $W_t(r,0)$ that we desire, we can get essentially ingoing (propagating towards the origin) initial data just by making an appropriate choice for $W_t$ as a function of $W$ and $W_r$. The easiest way to achieve this is to approximate the equation of motion for W, by ignoring the self-interaction term $a\alpha W(1-W^2)/r^2$, and also assuming flat space: $a = 1$ and $\alpha = 1$. Then (2.15) becomes

$$W_{tt} = W_{rr}. \tag{2.28}$$

This is a Cartesian wave equation in spherical coordinates. One might expect a spherical wave equation, such as $(r\phi)_{tt} = (r\phi)_{rr}$, to describe spherically symmetric wavelike behaviour. However, this leads to $\phi$ and $\phi_r$ decaying to 0 as $r \to \infty$. Usually this leads to a falloff in energy density (or related quantity) at large distances away from the origin. However, the energy density $\rho$ in this case is proportional to $(1 - W^2)^2$, so a spherical wave equation for $W$ at large radii would not lead to the expected falloff of energy density at large radii. This approximation lets us capture the wave-like nature of $W$. In particular it allows us to write an exactly ingoing solution to this approximated equation, simply $W = W_o(t + r)$. Then we can see that $W_t = W_o'$ and also $W_r = W_o'$. Then we have our approximately ingoing initial data by letting

$$W_t(r, 0) = W_r(r, 0). \tag{2.29}$$

Alternatively, the first order formulation makes it much easier to provide $\Pi$ at the initial time, rather than $W_t$. In this case $\Pi \approx W_t$ is assumed, so we can let

$$\Pi(r, 0) = \Phi(r, 0) = W_r(r, 0). \tag{2.30}$$

The initial profile of the system given by the initial data is also free for determination. We would like an initial distribution that yields the type I critical phenomena in which we are interested. Further details will be given in §4.1.

### 2.5.3 Boundary Conditions

Space is infinite in extent, but our computational resources are not. In particular, we cannot do numerical computations on a truly infinite spatial domain. Using a uniformly spaced discretization of the domain as we use in §3.1, we can only compute up to some finite radius. Thus, we must choose the largest radius, $r_{\max}$, that is sufficiently large so as not to significantly affect our results relative to the infinite-domain case.

However, stopping the simulation at some finite radius does make that radius special, and appropriate boundary conditions must be imposed to ensure that the behaviour of the fields there is essentially the same as for any point suitably far from the origin.

In the case of the collapse problem, we want to specify the initial matter profile that is collapsing. We also want the matter to be able to disperse to infinity, while at the same time having no Yang-Mills field enter into the problem from the outer boundary radius. So, in contrast to the case of the initial condition, we want the solution to be precisely outgoing at the outer

boundary. Again, the wave-like nature of our field makes a clear decomposition of solutions into ingoing and outgoing parts. This is only approximately true, since the self-interaction potential and gravitational field can cause the field to backscatter at any finite radius. For large enough radius, though, this effect is minimal. So, at the outer boundary, we assume a large enough radius $r_{\max}$ so that $a = \alpha = 1$ and $W(1-W^2)/r^2 \approx 0$, so that we again have $W_{tt} = W_{rr}$. This has a purely outgoing solution $W = W_1(t-r)$; at the outer boundary, then, $W_t = W_1'$ and $W_r = -W_1'$. So the outer boundary condition following from this approximation, is

$$W_t(r_{\max}, t) + W_r(r_{\max}, t) = 0. \tag{2.31}$$

Since $a$ and $\alpha$ are described by first order ODEs, they require only one boundary condition each. The condition on $a$ has already been treated, giving regularity at the origin. We are in fact free to choose a boundary condition for $\alpha$. If we want the time variable $t$ to be the time measured by a stationary observer at infinity, we can use our choice of coordinates to require

$$\lim_{r\to\infty} \alpha(r,t) = \frac{1}{a(r,t)}. \tag{2.32}$$

This follows from the well-known and unique Schwarzschild form

$$ds^2 = -\left(1 - \frac{2M}{r}\right) dt^2 + \left(1 - \frac{2M}{r}\right)^{-1} dr^2 + r^2 d\Omega^2 \tag{2.33}$$

for any piece of vacuum spacetime in spherical symmetry. Here the $t$ coordinate measures the time for a stationary observer at infinity. Matching these forms as $r \to \infty$, we immediately recover (2.32).

For the first order formulation, we note that

$$(W_r)_{tt} = W_{rtt} = W_{ttr} = (W_{tt})_r = (W_{rr})_r = (W_r)_{rr} \tag{2.34}$$

$$(W_t)_{tt} = (W_{tt})_t = (W_{rr})_t = W_{rrt} = W_{trr} = (W_t)_{rr}, \tag{2.35}$$

and since $\Phi = W_r$ and $\Pi = W_t$ under the large $r$ approximation, both $\Phi$ and $\Pi$ satisfy the Cartesian wave equation. So the same argument yields outgoing boundary conditions for them:

$$\Phi_t(r_{\max}, r) + \Phi_r(r_{\max}, r) = 0 \tag{2.36}$$

$$\Pi_t(r_{\max}, r) + \Pi_r(r_{\max}, r) = 0. \tag{2.37}$$

# Chapter 3

# Finite Difference Approximations

## 3.1 Terminology

The goal of finite difference approximation is to approximate some differential system

$$Lu - f = 0 \tag{3.1}$$

with a corresponding finite difference system

$$L^h u^h - f^h = 0. \tag{3.2}$$

Here $L$ is some differential operator acting on the solution $u$ and $f$ is some function defined on the domain $D$ of the problem. This work considers problems with at most one spatial and temporal dimension. We cover the domain $D$ with a grid $G$, choosing uniform spatial spacing $\Delta r \equiv h$ and uniform temporal spacing $\Delta t \equiv \lambda h$ between grid points, where $\lambda$ is known as the *Courant number*. Then $f^h$ is the function $f$ evaluated on $G$, $L^h$ is the finite difference approximation of $L$ on $G$, and $u^h$ is the discrete solution. Since $u^h$ is a discrete solution, we introduce the notation $u_j \equiv u^h(r_j)$ for one-dimensional problems dependent on the spatial variable $r$, and $u_j^n \equiv u^h(r_j, t^n)$ for problems also dependent on the temporal variable $t$. If the spatial domain is $[r_{\min},r_{\max}]$ and the temporal domain $[0,t^{\max}]$, then $r_j = r_{\min} + jh$ and $t^n = j\lambda h$ are the locations of the grid points. $x^\mu$ will be used to denote the spacetime coordinates $(r,t)$. See figure 3.1 for an example of a uniform grid on a spatial and temporal domain and the grid point labelling convention. Referring to a system at *time level* $n$ means to consider the system at time $t = t^n$; this terminology appears often when solving time-evolution PDEs. These discretizations are known collectively as a finite difference approximation (FDA).

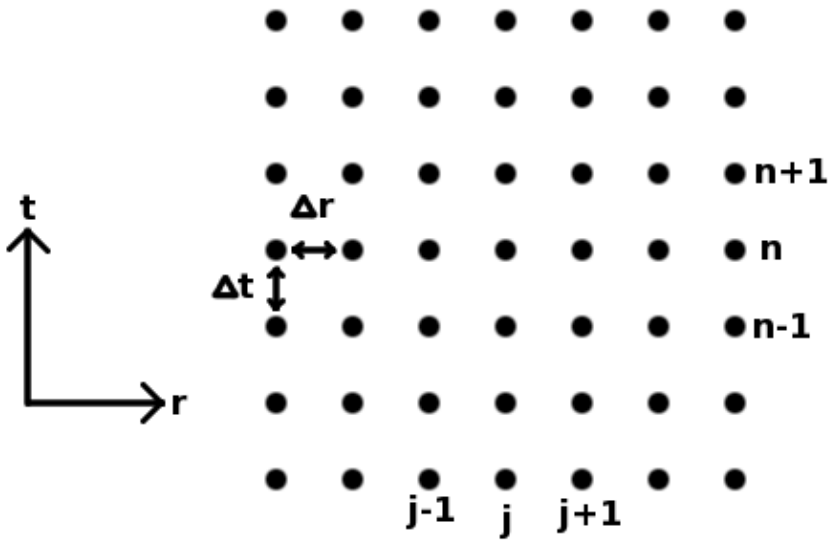


Figure 3.1: Portion of a uniform grid on the temporal and spatial domains. Spacings in $t$ and $r$ are both uniform, but need to be equal. The value of the $j^{\text{th}}$ spatial grid point is given by $r_j$, while the value of the $n^{\text{th}}$ temporal grid point is given by $t^n$. At the grid points, we define $u_j^n \equiv u^h(r_j, t^n)$.

The approximate solution converges to the continuum solution if

$$\lim_{h\to 0} u^h = u, \tag{3.3}$$

which is the hope in writing any finite-difference approximation.

Often the solution of (3.2) is difficult or impossible to obtain algebraically, and iterative methods must be used. In this case the approximation to the continuum solution, $\tilde{u}^h$, leads to a *residual* $r^h = L^h\tilde{u}^h - f^h$ which we wish to drive to 0 to obtain the discrete solution $u^h$.

The *truncation error* $\tau^h$ is defined by

$$\tau^h = L^h u - f^h, \tag{3.4}$$

and is a measure of the error produced by the discretization of $L$ and $f$. The solution error $e^h = u - u^h$ is then expected to be related to the truncation error, in terms of the level of accuracy obtained by the particular differencing approximation.

We say that the particular FDA is $m^{\text{th}}$ *order (accurate)* if we have

$$\lim_{h\to 0} \tau^h = O(h^m); \tag{3.5}$$

that is, $m$ is an integer giving the leading power of $h$ in the truncation error.

## 3.2 Richardson Expansion

The truncation error $\tau^h$ can be made $m^{\text{th}}$ order accurate by an appropriate choice of the FDA. One would like to be able to use the order of accuracy of the truncation error to make some statement about the order of accuracy of the solution error, namely that the two errors are accurate to the same order in the grid spacing $h$.

The basis for analysis of the solution error lies in assuming the existence of a *Richardson expansion* for the discrete solution, namely

$$u^h(x^\mu) = u(x^\mu) + he_1(x^\mu) + h^2e_2(x^\mu) + \cdots \tag{3.6}$$

Now if the FDA is accurate to order $m$, then we have

$$\tau^h = h^m\tau_m(x^\mu) + O(h^{m+1}), \tag{3.7}$$

and since $u^h$ satisfies (3.2), applying the operator $L^h - f^h$ to (3.6) we have

$$0 = h^m\tau_m(x^\mu)+O(h^{m+1})+hL^he_1(x^\mu)+\cdots+h^mL^he_m(x^\mu)+O(h^{m+1}). \tag{3.8}$$

This assumes that $L$ and $L^h$ are linear, but this argument can be expanded to the non-linear case.

Now this means that $L^h e_i(x^\mu) = 0$ in order that (3.8) is satisfied for all orders of $h$, for $1 \leq i \leq m-1$. But noting that $e_i(x^\mu)$ is $h$-independent, this cannot be true for a general $h$ unless we have the trivial solution $e_i(x^\mu) = 0$. This yields the result that if the FDA is accurate to order $m$, then we have that *solution error* $e^h(x^\mu) = u^h(x) - u(x^\mu)$ is $O(h^m)$, since

$$u^h(x^\mu) = u(x) + h^m e_m(x^\mu) + h^{m+1} e_{m+1}(x^\mu) + \cdots . \tag{3.9}$$

## 3.3 Convergence Testing

We need some way to test that the FDA solution $u^h$ actually is converging as $h \to 0$. We again make use of the Richardson expansion (3.6). What is needed is a diagnostic quantity that can be used to compare various $u^{h_i}$ for smaller and smaller $h_i$. To this end we consider a base grid spacing $h$ and look at $u^h$, $u^{2h}$ and $u^{4h}$, which we expect to look like

$$\begin{aligned} u^h(x^\mu) &= u(x^\mu) + he_1(x) + h^2 e_2(x^\mu) + \cdots \\ u^{2h}(x^\mu) &= u(x^\mu) + 2he_1(x) + (2h)^2 e_2(x^\mu) + \cdots \\ u^{4h}(x^\mu) &= u(x^\mu) + 4he_1(x) + (4h)^2 e_2(x^\mu) + \cdots \end{aligned}$$

in the limit that $h \to 0$. Then we can look at the differences

$$\begin{aligned} u^{4h}(x^\mu) - u^{2h}(x^\mu) &= 2he_1(x^\mu) + 12h^2 e_2(x^\mu) + \cdots \qquad (3.10) \\ &+ (4^n - 2^n)h^n e_n(x^\mu) + \cdots \\ u^{2h}(x^\mu) - u^h(x^\mu) &= he_1(x^\mu) + 3h^2 e_2(x^\mu) + \cdots \qquad (3.11) \\ &+ (2^n - 1)h^n e_n(x^\mu) + \cdots \end{aligned}$$

If our FDA is $m^{\text{th}}$ order accurate, then we have $e_1(x^\mu) = \cdots = e_{m-1}(x^\mu) = 0$, so the quantity

$$\begin{aligned} C^h(x^\mu) = \frac{u^{4h}(x^\mu) - u^{2h}(x^\mu)}{u^{2h}(x^\mu) - u^h(x^\mu)} &= \frac{2^m + \frac{(4^{m+1}-2^{m+1})h^{m+1}e_{m+1}(x^\mu)}{(2^m-1)h^m e_m(x^\mu)} + \cdots}{1 + \frac{(2^{m+1}-1)h^{m+1}e_{m+1}(x^\mu)}{(2^m-1)h^m e_m(x^\mu)} + \cdots} \\ &= \frac{2^m + h\frac{(4^{m+1}-2^{m+1})e_{m+1}(x^\mu)}{(2^m-1)e_m(x^\mu)} + \cdots}{1 + h\frac{(2^{m+1}-1)e_{m+1}(x^\mu)}{(2^m-1)e_m(x^\mu)} + \cdots} \end{aligned} \tag{3.12}$$

after cancelling the common factor of $(2^m - 1)h^m e_m(x^\mu)$. From this, we can easily see that

$$\lim_{h\to 0} C^h(x^\mu) = 2^m. \tag{3.13}$$

If this behaviour is seen in $u^h$, then it is strong indication that $u^h$ is converging as $h \to 0$, and this furthermore can give the order of accuracy of our FDA scheme. It is a strong indication that $u^h$ indeed has an expansion in $h$, with the lowest order error term being of order $m$.

### 3.3.1 Practical Convergence Testing

In practice, it may be more useful to consider the function

$$\frac{u^{2kh}(x^\mu) - u^{kh}(x^\mu)}{(2^m - 1)k^m h^m} = e_m(x^\mu) + \frac{2^{m+1} - 1}{2^m - 1} khe_{m+1}(x^\mu) + O(h^2), \tag{3.14}$$

and compare the results for $k = 1, 2, \ldots, N$,$N$ different grid spacings. These should all be fairly close to one another, being $e_m(x^\mu)$ up to $O(h)$ terms, and the similarity should improve as the lowest grid spacing $h \to 0$.

## 3.4 Discretizations

A finite difference operator, $L^h$, is a weighted sum of the discretized solution $u^h$. In the one-dimensional single function case we may write this as

$$L^h u_i = \ldots + a_{-1}u_{i-1} + a_0 u_i + a_1 u_{i+1} + \ldots \tag{3.15}$$

with $a_n$ constants depending on $L^h$. If we assume a Taylor expansion of $u$ about $x_i$, then after replacing the $u_n$ in (3.15) by the expansion of $u$ evaluated at $x_n$, and rearranging terms, we get

$$\begin{aligned} Lu_i &= u\,(\ldots + a_{-1} + a_0 + a_1 + \ldots) \\ &+ u'h\,(\ldots - 2a_{-2} - a_{-1} + a_1 + 2a_2 + \ldots) \\ &+ u''\frac{h^2}{2}\left(\ldots + 2^2 a_{-2} + a_{-1} + a_1 + 2^2 a_2 + \ldots\right) + \ldots \\ &+ u^{(n)}\frac{h^n}{n!}\,(\ldots + (-2)^n a_{-2} + (-1)^n a_{-1} + a_1 + 2^n a_2 + \ldots) \\ &+ \ldots \end{aligned} \tag{3.16}$$

From this, one may make appropriate choices of the $a_n$ in order to obtain the $k^{\text{th}}$ order derivative by letting the sum of coefficients in front of $u'$, ... , $u^{(k-1)}$ to be 0, and the sum of coefficients in front of $u^{(k)}$ to be $k!/h^k$.

| Function | CentrePoint | Discretization | Order | |
|---|---|---|---|---|
| $u'$ | $x_j$ | $\frac{u_{j+1} - u_{j-1}}{2h}$ | $h^2$ | (3.17) |
| $u'$ | $x_{j+\frac{1}{2}}$ | $\frac{u_{j+1} - u_j}{h}$ | $h^2$ | (3.18) |
| $u'$ | $x_j$ | $\frac{3u_j - 4u_{j-1} + u_{j-2}}{2h}$ | $h^2$ | (3.19) |

Table 3.1: Table of Commonly Used Discretizations

In general it is difficult to accomplish this unless all of the coefficients $a_n$ are of the same order in $h$. In the case of the $k^{th}$ derivative, this is $O(h^{-k})$. Then we can get the $k^{\text{th}}$ derivative to $O(h^m)$ by requiring the coefficients in front of $u^{(k+1)}, \ldots, u^{(k+m-1)}$ to be 0. Then $Lu_i = u_i^{(k)} + O(h^m)$.

## 3.5 Constructing Discretized Differential Operators

Most differential operators involve some linear combination of multiple derivatives of certain quantities, which may themselves involve derivatives. It is thus possible most of the time to simply 'build up' the discretized differential operator from discretizations of the derivative at certain points.

The first derivative requires only two pieces of information, and has two generally useful discretizations, which differ in their centre point, the point about which we perform the Taylor expansion. Table 3.1 lists some of the more commonly used discretizations.

For example, we will confirm that $(u_{j+1} - u_j)/h$ is an $O(h^2)$ accurate discretization for $u'_{j+\frac{1}{2}}$. Writing out each term as a Taylor expansion from the centre point of the scheme, we have

$$\begin{aligned}
\frac{u_{j+1} - u_j}{h} &= \frac{u_{j+\frac{1}{2}} + \frac{h}{2}u'_{j+\frac{1}{2}} + \left(\frac{h}{2}\right)^2 u''_{j+\frac{1}{2}} + O(h^3)}{h} \\
&- \frac{u_{j+\frac{1}{2}} - \frac{h}{2}u'_{j+\frac{1}{2}} + \left(\frac{h}{2}\right)^2 u''_{j+\frac{1}{2}} + O(h^3)}{h} \\
&= \frac{2\left(\frac{h}{2}\right) u'_{j+\frac{1}{2}} + O(h^3)}{h} = u'_{j+\frac{1}{2}} + O(h^2). \qquad (3.20)
\end{aligned}$$

Since the discretization $(u_{j+1} - u_{j-1})/2h$ is the same as the above under the linear transformation $j + \frac{1}{2} \to j$, $h \to 2h$, we see it is an $O(h^2)$ discretization for $u'_j$.

Taking derivatives at boundaries is a more difficult task, since one only has access to grid points on one side of the current point. In this case a backwards $O(h^2)$ approximation for the derivative is given by

$$\begin{aligned} & \frac{3u_j - 4u_{j-1} + u_{j-2}}{2h} \\ = & \frac{3u_j - 4\left(u_j - hu'_j + \frac{h^2}{2}u''_j + O(h^3)\right) + \left(u_j - 2hu'_j + \frac{(2h)^2}{2}u''_j + O(h^3)\right)}{2h} \\ = & \frac{(3-4+1)u_j + (4-2)hu'_j - (4-4)\frac{h^2}{2}u''(j) + O(h^3)}{2h} \\ = & u'_j + O(h^2). \end{aligned} \tag{3.21}$$

In some cases an $O(h)$ backwards derivative suffices, in which case we may use only the neighbouring point, giving

$$\frac{u_j - u_{j-1}}{h} = \frac{u_j - \left(u_j - hu'_j + O(h^2)\right)}{h} = u'_j + O(h). \tag{3.22}$$

### 3.5.1 Discretizations Not Centred At Grid Points

Consider the *linear* differential system $L^h u^h - f^h = 0$. Suppose that we have a discretization of $L^h$ that is centred at the spatial point $x_{j+\frac{1}{2}} = (x_j + x_{j+1})/2$, and which is furthermore an $O(h^2)$ discretization. If in this discretization the value $u_{j+\frac{1}{2}}$ must be evaluated, then we only actually need an $O(h^2)$ approximation to $u_{j+\frac{1}{2}}$. Since the system is linear, this $O(h^2)$ term will be acted on by $L^h$, still being second-order in $h$, and add to the $O(h^2)$ terms arising from the approximation of $L$ by $L^h$.

In our calculations most half-centred discretizations of the differential $L^h u^h$ do not involve the value $u_{j+\frac{1}{2}}$; instead, $u_{j+\frac{1}{2}}$ appears only in the evaluation of $f$ at the point where the differential system is being evaluated, namely $x_{j+\frac{1}{2}}$. In this case it is even clearer that the whole system is only affected by an error of $O(h^2)$, since

$$\begin{aligned} f(u_{j+\frac{1}{2}} + e_u h^2, x_{j+\frac{1}{2}}) &= f(u_{j+\frac{1}{2}}, x_{j+\frac{1}{2}}) + h^2 e_u f_u(u_{j+\frac{1}{2}}, x_{j+\frac{1}{2}}) \\ &+ \frac{(h^2 e_u)^2}{2!} f_u u(u_{j+\frac{1}{2}}, x_{j+\frac{1}{2}}) + \cdots . \end{aligned} \tag{3.23}$$

To this end the average value of $u$ suffices, since

$$\begin{aligned}\frac{u_{j+1}+u_j}{2} &= \frac{1}{2}\left(\left(u_{j+\frac{1}{2}}+\frac{h}{2}u'_{j+\frac{1}{2}}+O(h^2)\right)+\left(u_{j+\frac{1}{2}}-\frac{h}{2}u'_{j+\frac{1}{2}}+O(h^2)\right)\right)\\ &= u_{j+\frac{1}{2}}+O(h^2).\end{aligned} \tag{3.24}$$

Now consider a differential system with two functions, $u$ and $v$, that need evaluation at a half-step and assume that we need some $O(h^2)$ approximation of

$$g\left(u_{j+\frac{1}{2}}, v_{j+\frac{1}{2}}, x_{j+\frac{1}{2}}\right). \tag{3.25}$$

It turns out that the average of $g$ suffices to obtain an $O(h^2)$ approximation:

$$\begin{aligned}&\frac{1}{2}(g(u_{j+1},v_{j+1},x_{j+1})+g(u_j,v_j,x_j))\\ =\ &\frac{1}{2}\left(\left(g(u_{j+\frac{1}{2}},v_{j+\frac{1}{2}},x_{j+\frac{1}{2}})+(g_u u'+g_v v'+g_x)\big|_{x_{j+\frac{1}{2}}}\frac{h}{2}+O(h^2)\right)\right.\\ +\ &\left.\left(g(u_{j+\frac{1}{2}},v_{j+\frac{1}{2}},x_{j+\frac{1}{2}})-(g_u u'+g_v v'+g_x)\big|_{x_{j+\frac{1}{2}}}\frac{h}{2}+O(h^2)\right)\right)\\ =\ &g\left(u_{j+\frac{1}{2}},v_{j+\frac{1}{2}}\right)+O(h^2).\end{aligned} \tag{3.26}$$

Additionally, one may need an initial guess for the value of a function at some grid point where earlier function values are known, in order to start some iterative scheme. In this case the same reasoning may be applied to show that the linear extrapolation gives an $O(h^2)$ approximation:

$$\begin{aligned}2u_j-u_{j-1} &= 2\left(u_{j+1}-hu'_{j+1}+O(h^2)\right)\\ &- \left(u_{j+1}-2hu'_{j+1}+O(h^2)\right)=u_{j+1}+O(h^2).\end{aligned} \tag{3.27}$$

### 3.5.2 Numerical Integration of Ordinary Differential Equations

Consider the situation of a differential system that reduces to a first-order ODE for one function $u \equiv u(x)$,

$$u' = f(u,x), \tag{3.28}$$

as is the case for $a$ and $\alpha$ as seen in §2.4. This can be discretized as

$$\frac{u_{j+1}-u_j}{h} = f(u_{j+\frac{1}{2}}, x_{j+\frac{1}{2}}), \tag{3.29}$$

which retains $O(h^2)$ accuracy upon using the average value for $u_{j+\frac{1}{2}}$. Then the approximate discrete system becomes

$$\frac{u_{j+1}-u_j}{h} = f\left(\frac{u_{j+1}+u_j}{2}, x_{j+\frac{1}{2}}\right) = f(u_j, u_{j+1}, x_{j+\frac{1}{2}}), \tag{3.30}$$

which is simply a (possibly nonlinear) algebraic equation for $u_{j+1}$ in terms of $u_j$, or vice-versa. From this, one may obtain $u_{j+1}$ from $u_j$, or vice-versa, thus allowing forwards or backwards integration of the ODE.

### 3.5.3 Discretizing Multiple Derivatives

Discretizing multiple derivatives can be accomplished by "nesting" the discretizations of lower-order derivatives. Consider the following $O(h^2)$ approximation for $v'$: $(v_{j+\frac{1}{2}} - v_{j-\frac{1}{2}})/h$. This is merely the discretization introduced in (3.18), shifted by half a grid point. Not knowing $v$ in between grid points, we would need to use averages to make a further $O(h^2)$ approximation, which would yield the old discretization for $v'$ given in (3.17).

However, suppose we instead wanted the second derivative of the function $u$, so letting $v = u'$ gets $v' = u''$. In this case we can make use of the discretization for $u'$ at the half grid points, so that we are lead to the discretization

$$\frac{v_{j+\frac{1}{2}} - v_{j-\frac{1}{2}}}{h} = \frac{(u_{j+1}-u_j)-(u_j-u_{j-1})}{h^2} = \frac{u_{j+1}-2u_j+u_{j-1}}{h^2}. \tag{3.31}$$

This leads us to an $O(h^2)$ discretization of $(gu')'$ for some function $g$, namely

$$\frac{(g_{j+1}+g_j)(u_{j+1}-u_j)-(g_j+g_{j-1})(u_j-u_{j-1})}{2h^2}. \tag{3.32}$$

Now, we have the following expansions:

$$g_j + g_{j+1} = 2g_j + hg_j' + \frac{h^2}{2}g_j'' + \frac{h^3}{6}g_j''' + O(h^4) \tag{3.33}$$

$$g_j + g_{j-1} = 2g_j - hg_j' + \frac{h^2}{2}g_j'' - \frac{h^3}{6}g_j''' + O(h^4) \tag{3.34}$$

$$-u_j + u_{j+1} = hu_j' + \frac{h^2}{2}u_j'' + \frac{h^3}{6}u_j''' + O(h^4) \tag{3.35}$$

$$u_j - u_{j-1} = hu_j' - \frac{h^2}{2}u_j'' + \frac{h^3}{6}u_j''' + O(h^4). \tag{3.36}$$

We then have

$$\begin{aligned}(g_j + g_{j+1})(u_{j+1} - u_j) &= h(2g_j u_j) + h^2(g_j u_j'' + g_j' u_j') \\ + \quad h^3 &\left(\frac{1}{2}g_j'' u_j + \frac{1}{2}g_j' u_j'' + \frac{1}{3}g_j u_j'''\right) + O(h^4) \qquad (3.37) \\ (g_j + g_{j-1})(u_j - u_{j-1}) &= h(2g_j u_j) + h^2(-g_j u_j'' - g_j' u_j') \\ + \quad h^3 &\left(\frac{1}{2}g_j'' u_j + \frac{1}{2}g_j' u_j'' + \frac{1}{3}g_j u_j'''\right) + O(h^4). \qquad (3.38)\end{aligned}$$

Thus, we have that our discretization is

$$\begin{aligned}&\frac{(g_{j+1} + g_j)(u_{j+1} - u_j) - (g_j + g_{j-1})(u_j - u_{j-1})}{2h^2} \\ = \quad &\frac{h(0) + h^2(2g_j u_j'' + 2g_j' u_j') + h^3(0) + O(h^4)}{2h^2} \\ = \quad &g_j u_j'' + g_j' u_j' + O(h^2) = (g_j u_j')_j' + O(h^2) \qquad (3.39)\end{aligned}$$

by the product rule.

## 3.6 Stability and the Courant Number

For a finite difference scheme to be stable, it must not contain any modes that grow without bound when the continuum solution itself does not have this behaviour. One such criterion for the difference schemes used in this work is the condition that the Courant number

$$\lambda \leq 1. \qquad (3.40)$$

This is known as the CFL condition, from Courant, Friedrichs and Lewy [10]. Since we are working with units with $c = 1$, information may propagate at speed 1. This condition roughly states that the numerical domain of dependence must contain the physical domain of dependence. See Figure 3.2 for an illustration.

## 3.7 Solving Discretized Systems

In general, there are two types of equations that need to be solved in order to obtain the time evolution of the systems of partial differential equations considered here. The first are *evolution equations*, ones involving time derivatives of the functions involved. The second are *constraint equations*,

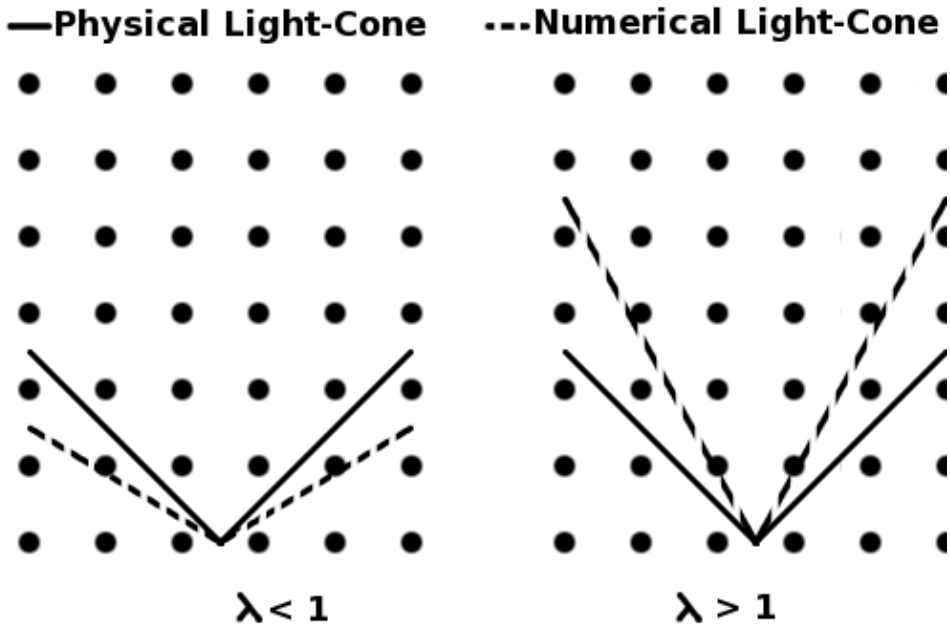


Figure 3.2: Light-cones (domains of spacetime causal dependence) for the physical problem (with speed of propagation 1) and the numerical problem (with speed of propagation $\lambda$, since neighbouring grid points are used at the previous time level). Values of $\lambda > 1$ yield grid points that do not depend numerically on grid points that they would physically depend on. This fails to capture all of the physics, and leads to instabilities. Values of $\lambda < 1$ always contain the physical light-cone within the numerical one, so the 'information' from a grid point will always reach the grid points it is physically able to. Equally spaced grid points are shown for reference.

which are purely ordinary differential equations, in the radial coordinate $r$, that must be satisfied at all times.

By using a discretized approximation to an evolution equation, one ends up with a system of algebraic equations. We look to solve for the values of the functions at time level $n+1$ based on values already determined at time level $n$ (and $n-1$, depending on the nature of the scheme). This is accomplished through the use of pointwise Newton-Gauss-Seidel relaxation. For any function $u$ given by an evolution equation, its value $u_j^{n+1}$ is given implicitly in the discretized version of the evolution equation applied at the position $r_j$. So for each position point $r_j$ we can associate to each unknowns at the advanced time level $n+1$ (such as $u_j^{n+1}$) the equation (likely implicitly) defining it. Newton-Gauss-Seidel relaxation visits all the grid points at time level $n+1$ in some prescribed order, at each point updating the value of $u_j^{n+1}$ using the associated equation; once all positions are updated, this process (a 'pass-through') is repeated until there is sufficiently small change from the update. The value at a grid point is updated by solving the associated discretized evolution equation using Newton's method. The Gauss-Seidel method differs from others in that function values from the current update are used to update other positions that have not yet been visited in the current pass-through. Rapid Numerical Prototyping Language (RNPL) was used to implement this technique automatically, given the relevant discretized evolution equations and boundary conditions.

In this way, the discretized equations can be satisfied to yield function values at the advanced time levels for the functions given by evolution equations. Then those functions that are determined by the constraint equations can be determined through usual methods of solving ordinary differential equations, which in this work will consist of integration using finite difference techniques as described previously.

In some cases, a function that is determined by a constraint equation may appear evaluated at the advanced time level. In this case, the evolution and constraint equations become coupled, and then must be repeatedly solved iteratively until all are satisfied simultaneously. This iterative technique is also used in the case where the constraint equations cannot be decoupled.

## 3.8 Discretization of the First Order Equations of Motion

We have the first order equations of motion

$$\Phi_t = \left(\frac{\alpha}{a}\Pi\right)_r \tag{3.41}$$

$$\Pi_t = \left(\frac{\alpha}{a}\Phi\right)_r + \frac{a\alpha}{r^2}W(1-W^2) \tag{3.42}$$

$$\frac{a_r}{a} + \frac{a^2-1}{r^2} - \frac{1}{r}\left(\Phi^2 + \Pi^2 + \frac{a^2}{2r^2}(1-W^2)^2\right) = 0 \tag{3.43}$$

$$\frac{\alpha_r}{\alpha} - \frac{a^2-1}{r^2} - \frac{1}{r}\left(\Phi^2 + \Pi^2 - \frac{a^2}{2r^2}(1-W^2)^2\right) = 0, \tag{3.44}$$

where

$$\Phi = W_r, \tag{3.45}$$

$$\Pi = \frac{a}{\alpha}W_t, \tag{3.46}$$

so that

$$W(r,t) = W_0 + \int_0^r \Phi(x,t)dx \tag{3.47}$$

describes the Yang-Mills field variable $W$.

We introduce a discretization of these equations by centering the scheme at time level $n+\frac{1}{2}$. Then (3.41) becomes

$$\frac{\Phi_j^{n+1} - \Phi_j^n}{\Delta t} = \frac{\left(\frac{\alpha}{a}\Pi\right)_{j+1}^{n+\frac{1}{2}} - \left(\frac{\alpha}{a}\Pi\right)_{j-1}^{n+\frac{1}{2}}}{2\Delta r} \tag{3.48}$$

for points $r_j$ in the interior of the grid, and (3.42) similarly becomes

$$\frac{\Pi_j^{n+1} - \Pi_j^n}{\Delta t} = \frac{\left(\frac{\alpha}{a}\Phi\right)_{j+1}^{n+\frac{1}{2}} - \left(\frac{\alpha}{a}\Phi\right)_{j-1}^{n+\frac{1}{2}}}{2\Delta r} + \left(\frac{\alpha a}{r^2}W(1-W^2)\right)_j^{n+\frac{1}{2}}. \tag{3.49}$$

At this point, we need to provide values for the half time level. Since the average value of a function over the two time levels gives an $O(h^2)$ approximation to this, we have the discretizations

$$\frac{\Phi_j^{n+1}-\Phi_j^n}{\Delta t} = \frac{\left(\frac{\alpha}{a}\Pi\right)_{j+1}^{n+1}+\left(\frac{\alpha}{a}\Pi\right)_{j+1}^{n}-\left(\frac{\alpha}{a}\Pi\right)_{j-1}^{n+1}-\left(\frac{\alpha}{a}\Pi\right)_{j-1}^{n}}{4\Delta r} \quad (3.50)$$

$$\frac{\Pi_j^{n+1}-\Pi_j^n}{\Delta t} = \frac{\left(\frac{\alpha}{a}\Phi\right)_{j+1}^{n+1}+\left(\frac{\alpha}{a}\Phi\right)_{j+1}^{n}-\left(\frac{\alpha}{a}\Phi\right)_{j-1}^{n+1}-\left(\frac{\alpha}{a}\Phi\right)_{j-1}^{n}}{4\Delta r} + \frac{\left(\left(\frac{\alpha a}{r^2}W(1-W^2)\right)_j^{n+1}+\left(\frac{\alpha a}{r^2}W(1-W^2)\right)_j^{n}\right)}{2}. \quad (3.51)$$

These are $O(h^2)$ approximations to (3.41) and (3.42), evaluated at the point $(r_j, t^{n+\frac{1}{2}})$, providing discrete evolution equations for $\Phi$ and $\Pi$.

After (3.50) and (3.51), along with the appropriate boundary conditions, are solved to produce $\Phi^{n+1}$ and $\Pi^{n+1}$, then (3.47), (3.43) and (3.44) are ODEs that can be solved by the numerical integration method described in §3.5.2. This yields $W, a$ and $\alpha$ at time level $n+1$. The evolution for this time step is then complete.

### 3.8.1 Boundary and Regularity Conditions

We need to apply the boundary and regularity conditions

$$\Phi_t(r_{\max})+\Phi_r(r_{\max})=0 \quad \Pi_t(r_{\max})+\Pi_r(r_{\max})=0 \quad (3.52)$$

$$W(0)=1 \quad \Phi(0)=0 \quad \Pi(0)=0 \quad (3.53)$$

$$a(0)=1 \quad \alpha(r_{\max})=\frac{1}{a(r_{\max})} \quad (3.54)$$

with the appropriate discretizations on the grid. Now, (3.54) simply gives initial conditions for the numerical integration of the constraint ODEs, while (3.53) gives the constant values of $W$, $\Phi$, and $\Pi$ at the first grid point. (3.52) can be discretized to $O(h^2)$ at the half-time level to obtain

$$\frac{3\Phi_N^{n+1}-4\Phi_{N-1}^{n+1}+\Phi_{N-2}^{n+1}+3\Phi_N^n-4\Phi_{N-1}^n+\Phi_{N-2}^n}{4\Delta r}=\frac{\Phi_N^{n+1}-\Phi_N^n}{\Delta t} \quad (3.55)$$

$$\frac{3\Pi_N^{n+1}-4\Pi_{N-1}^{n+1}+\Pi_{N-2}^{n+1}+3\Pi_N^n-4\Pi_{N-1}^n+\Pi_{N-2}^n}{4\Delta r}=\frac{\Pi_N^{n+1}-\Pi_N^n}{\Delta t} \quad (3.56)$$

at the last grid point, $r_N$, using time averaged difference equations to yield $O(h^2)$ accuracy.

## 3.9 Discretization of the Second Order Equations of Motion

We have the second order equations of motion

$$\left(\frac{a}{\alpha}W_t\right)_t = \left(\frac{\alpha}{a}W_r\right)_r + \frac{a\alpha}{r^2}W(1-W^2) \tag{3.57}$$

$$\begin{aligned} & \frac{a_r}{a} + \frac{a^2-1}{r^2} \\ -\frac{1}{r}\left(W_r^2 + \frac{a^2}{\alpha^2}W_t^2 + \frac{a^2}{2r^2}(1-W^2)^2\right) &= 0 \end{aligned} \tag{3.58}$$

$$\begin{aligned} & \frac{\alpha_r}{\alpha} - \frac{a^2-1}{r^2} \\ -\frac{1}{r}\left(W_r^2 + \frac{a^2}{\alpha^2}W_t^2 - \frac{a^2}{2r^2}(1-W^2)^2\right) &= 0, \end{aligned} \tag{3.59}$$

which only involve $W$ directly. The constraint equations for $a$ and $\alpha$ are solved using numerical integration as before. In this case both equations are now coupled, so they are solved iteratively, first for $a$ and then for $\alpha$. A first guess for $\alpha$ is given by linear extrapolation in time, $\alpha_j^{n+1} = 2\alpha_j^n - \alpha_j^{n-1}$. What is more difficult is the fact that $W_t$ is unknown — only $W$ is known — so we need an $O(h^2)$ discretization for $W_t$ in order to keep the discretization of the whole equation $O(h^2)$ accurate.

We choose to evaluate the constraint equations at time level $n+\frac{1}{2}$. As before, we use the time averages of discretizations at $t = t^n$ and $t = t^{n+1}$ to provide $O(h^2)$ accuracy at $t = t^{n+\frac{1}{2}}$. Then the discretization of (3.58) becomes

$$\begin{aligned} 0 &= \frac{a_{j+1}^{n+1} - a_j^{n+1} + a_{j+1}^n - a_j^n}{2\Delta t} \\ &+ \frac{1}{2}\left[\frac{a^3-a}{2r} - \frac{a}{r}\left(W_r^2 + \frac{a^2}{\alpha^2}W_t^2 + \frac{a^2}{2r^2}(1-W^2)^2\right)\right]_j^{n+1} \\ &+ \frac{1}{2}\left[\frac{a^3-a}{2r} - \frac{a}{r}\left(W_r^2 + \frac{a^2}{\alpha^2}W_t^2 + \frac{a^2}{2r^2}(1-W^2)^2\right)\right]_j^{n}, \end{aligned} \tag{3.60}$$

while the discretization of (3.59) becomes

$$\begin{aligned} 0 &= \frac{\alpha_{j+1}^{n+1} - \alpha_j^{n+1} + \alpha_{j+1}^n - \alpha_j^n}{2\Delta t} \\ &+ \frac{1}{2}\left[\frac{\alpha - \alpha a^2}{2r} - \frac{\alpha}{r}\left(W_r^2 + \frac{a^2}{\alpha^2}W_t^2 - \frac{a^2}{2r^2}(1-W^2)^2\right)\right]_j^{n+1} \\ &+ \frac{1}{2}\left[\frac{\alpha - \alpha a^2}{2r} - \frac{\alpha}{r}\left(W_r^2 + \frac{a^2}{\alpha^2}W_t^2 - \frac{a^2}{2r^2}(1-W^2)^2\right)\right]_j^{n}. \end{aligned} \quad (3.61)$$

Then (3.60) gives $a_{j+1}^{n+1}$ in terms of $a_j^{n+1}$, and other known values at time levels $n$ and $n+1$, allowing numerical integration to obtain $a^{n+1}$. Equation (3.61) similarly allows for numerical integration to obtain $\alpha^{n+1}$.

The differencing of (3.57) is fundamentally distinct from previous differencings, due to the existence of second spatial and time derivatives. Such discretizations require three pieces of information; hence, we will have a three-level scheme. The discretization of (3.57) will involve three separate time levels. We will make use of the discretization given by (3.32). In particular we have the final discretization of the equation of motion as

$$\begin{aligned} &\frac{\left(\left(\frac{a}{\alpha}\right)_j^{n+1} + \left(\frac{a}{\alpha}\right)_j^n\right)\left(W_j^{n+1} - W_j^n\right) - \left(\left(\frac{a}{\alpha}\right)_j^n + \left(\frac{a}{\alpha}\right)_j^{n-1}\right)\left(W_j^n - W_j^{n-1}\right)}{2\Delta t^2} \\ = &\frac{\left(\left(\frac{a}{\alpha}\right)_{j+1}^n + \left(\frac{a}{\alpha}\right)_j^n\right)\left(W_{j+1}^n - W_j^n\right) - \left(\left(\frac{a}{\alpha}\right)_j^n + \left(\frac{a}{\alpha}\right)_{j-1}^n\right)\left(W_j^n - W_{j-1}^n\right)}{2\Delta t^2} \\ + &\frac{\alpha_j^n a_j^n}{r_j} W_j^n\left(1 - (W_j^n)^2\right). \end{aligned} \quad (3.62)$$

### 3.9.1 Initial Conditions

With a three-level scheme, it is not sufficient merely to provide the value of $W$, $a$ and $\alpha$ at the initial time. One must provide them at a neighbouring time (usually at the *prior* time step). Since $a$ and $\alpha$ are governed by constraint equations at each time, this reduces to specifying $W$ at adjacent time level, which is equivalent to specifying the time derivative $W_t$ as well as $W$.

This must be done so that $W$ is obtained to $O(h^3)$ at the neighbouring time level. To get $O(h^2)$ accuracy at fixed finite $t_f$, we must have per-time-step accuracy of $O(h^3)$ since there are $O(h^{-1})$ time steps needed. This can be achieved through the use of the Taylor expansion of $W$ about $t = 0$,

namely

$$W(r,-\Delta t) = W(r,0) - \Delta t W_t(r,0) + \frac{\Delta t^2}{2} W_{tt}(r,0) + O(h^3). \tag{3.63}$$

Now, with initial data giving $W(r,0) = W_o(r)$ and $W_t(0,r) = V_o(r)$, $a$ and $\alpha$ can be determined as usual at the initial time. Then, $W_{tt}$ can be determined from the equation of motion for $W$, namely that

$$W_{tt}(r,0) = \frac{\alpha}{a}\left[\left(\frac{\alpha}{a}W_o'\right)' + \frac{\alpha}{a}W_o(1-W_o^2) - V_o\left(\frac{a}{\alpha}\right)_t\right]. \tag{3.64}$$

There is a distinct need for an iterative process here: the time derivative of $a/\alpha$ is required to compute $W_{tt}$, but there is no analytical expression for it. In this case, we need instead to use an approximation for it — an $O(h)$ approximation suffices, since to know $W$ to $O(h^3)$ we only need to know $W_{tt}$ to $O(h)$.

So, approximating $((a/\alpha)_t)_j^0$ with $\left[(a/\alpha)_j^0 - (a/\alpha)_j^{-1}\right]/\Delta t$, we see that we need to know $a$ and $\alpha$ at time level $-1$ to $O(h^2)$. In turn, to know *these*, we need not only $W^{-1}$, but also $W_t^{-1}$ to $O(h^2)$ in order to derive $a$ and $\alpha$ to $O(h^2)$. We can approximate the final unknown quantity, $W_t^{-1}$ by its Taylor expansion, $W_t(r,-\Delta t) = V_o(r) - \Delta t W_{tt}(r,0) + O(\Delta t^2)$.

Solving these equations iteratively yields $W_{tt}(r,0)$ to $O(h)$, $W_t^{-1}$ to $O(h^2)$, and $(a/\alpha)_t^0$ to $O(h)$, all of which yield $W^{-1}$ to $O(h^3)$.

### 3.9.2 Boundary and Regularity Conditions

The boundary and regularity conditions are of the exact same form as for the first-order equations:

$$W_t(r_{\max}) + W_r(r_{\max}) = 0 \qquad W(0) = 1 \tag{3.65}$$

$$a(0) = 1 \quad \alpha(r_{\max}) = \tfrac{1}{a(r_{\max})} \tag{3.66}$$

and are implemented and discretized in the exact same manner (see §3.8.1).

# Chapter 4

# Results

In this chapter we explore the results of the numerical simulations of gravitational critical phenomena using SU(2) fields. We first consider the traditional first order scheme. We will begin by showing evidence of type I critical phenomena, and follow it with convergence tests. Then a comparison with the second order scheme will be made; in general, the schemes agree quite well with a reasonable number of grid points.

## 4.1 Type I Critical Phenomena In SU(2) Yang-Mills Fields Using First Order Methods

For the initial data $W_o(r) = W(r, 0)$, we use a 'kink' form similar in form to a static solution discovered by Bartnik and McKinnon [4]. It has the form

$$W_o(r) = \frac{1 + \frac{r_o^2 - r^2}{\delta^2}}{\sqrt{\left(1 + \frac{r_o^2 - r^2}{\delta^2}\right)^2 + 4r^2}}, \tag{4.1}$$

with parameters $r_o$ and $\delta$. $r_o$ controls the center of the kink, where $W_o = 0$. $\delta$ controls the width of the kink, how quickly it transitions from $W_o$ near 1 to $-1$. Figure 4.1 shows the initial data $W_o(r)$ for $r_o = 15$ and $\delta = 2.0$.

Fixing $r_0 = 15$, we have a certain family of initial data that is parametrized by $\delta$. In this case $\delta^{-1}$ is the parameter that scales with the gravitational self-interaction of the system. Larger values of $\delta$ then correspond to the system dispersing to infinity for large times, ending up with flat space as the end state of evolution. Smaller values of $\delta$ will cause black hole creation.

See Figure 4.2 for a plot of the $W$ in the subcritical case: the system initially collapses inwards, but scatters through the origin, then disperses to infinity. Here, $\delta = 2.0$. Figure 4.3 shows a plot of the total mass contained in a given radius for the same case. Figure 4.4 shows $W$ for the supercritical case, where a black hole will be formed, with $\delta = 1.5$. The quantity $2m/r$ rapidly asymptotes to 1, indicating imminent black hole formation. This can be seen in figure 4.5. What is important to note here is that $2m/r$ is

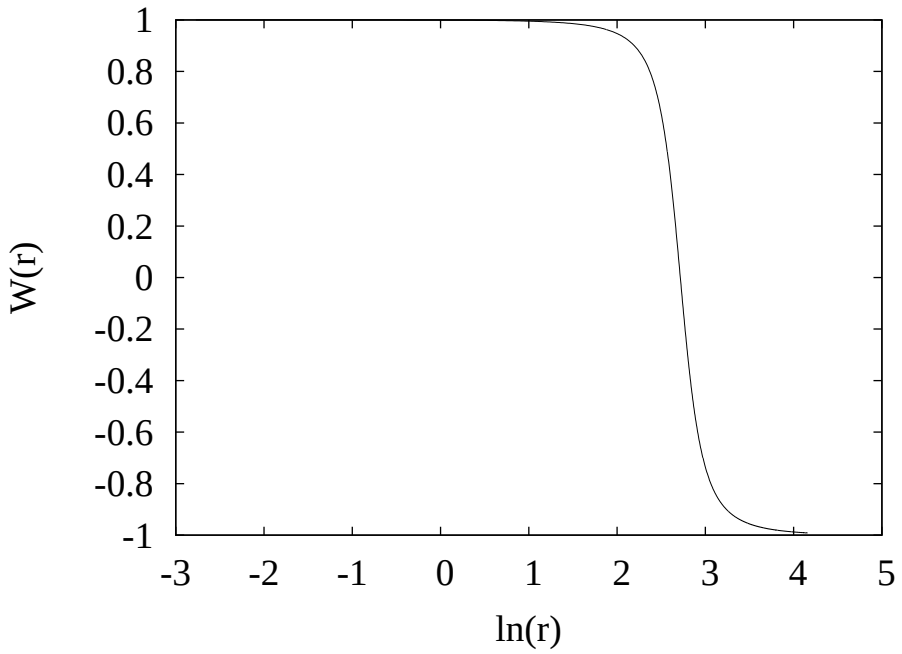


Figure 4.1: Initial profile for the Yang-Mills field variable $W$ as a function of ln(radius). Initial data for the field "velocity" is given by $\Pi \approx W_t = W_r$, as an approximation to precisely ingoing (towards the origin) initial motion.

asymptoting to 1 at some finite radius, $r_B$. So we immediately have a mass for the black hole formed, $m_B = r_B/2$, which we see is finite.

Finding the critical value of $\delta$ for this choice of $r_o$ can be accomplished using a bisection search. One starts with a range of $\delta$, $[\delta_1, \delta_2]$, where a black hole is formed for $\delta = \delta_1$, and flat space is reached for $\delta = \delta_2$. One then increases $\delta_1$ or descreases $\delta_2$ to their average value, $(\delta_1 + \delta_2)/2$, whichever keeps the same end state of the system for both $\delta_1$ and $\delta_2$. In this way, one can make the interval $[\delta_1, \delta_2]$ arbitrarily small, to the level of floating-point round-off error, thus obtaining a range for the critical value $\delta^*$, since $\delta_1 < \delta^* < \delta_2$. We perform this bisection search until $\delta^*$ is found to 16 significant figures, the level of floating-point precision.

Then with $\delta = 1.6566278489408265 \cong \delta^*$, we have a solution that is quite close to the critical solution. Further refinement of $\delta$ will not increase the precision of the critical parameter value due to the floating-point round-off error. Note that $\delta$ is known to much greater precision than it is likely to be accurate, in order to get as close as possible to the critical solution for this discretized problem at this specific grid spacing. The critical value of $\delta$ for the continuous problem will likely only be approximated to a few significant figures by this nonetheless finely tuned value for $\delta$. Nevertheless, with this value, Figure 4.7 shows the evolution of $W$ for this extremely-close-to-critical solution. Note that the solution settles in at a static solution and remains there for quite some time, illustrating that the critical solution truly is static. Figure 4.6 shows a comparison of the critical solution with a static solution discovered by Bartnik and McKinnon. The two agree quite well, and only differ significantly at large radii.

Figure 4.8 shows the quantity $2m/r$ for a slightly supercritical value of $\delta = 1.6566278489408260$. In this case, we have deliberately chosen a value of $\delta$ close to the critical value to show the creation of finite mass black holes and the discontinuous change in the end state of evolution on either side of the critical value of the parameter.

The last piece of critical behaviour is seen in the lifetime scaling. The solution lifetime is calculated by tracking where the variable $W$ crosses 0. The slope of this line, $\sigma$, is the family-independent parameter of interest. For the family of initial data with $r_o = 15$, $\sigma = 4.34294$. Setting $\delta = 1.66$ and varying $r_o$ yields another family of initial data. This has critical parameter value $r_o^* = 19.541136432698869$ and a value of $\sigma = 4.16923$. Figure 4.9 shows the solution lifetime as a function of $\ln|p - p^*|$, for the two families of initial data discussed above. Prior work on this same problem yielded a similar scaling parameter $\lambda = 0.5520$. Here, $\lambda$ is the equivalent of $\sigma$, except

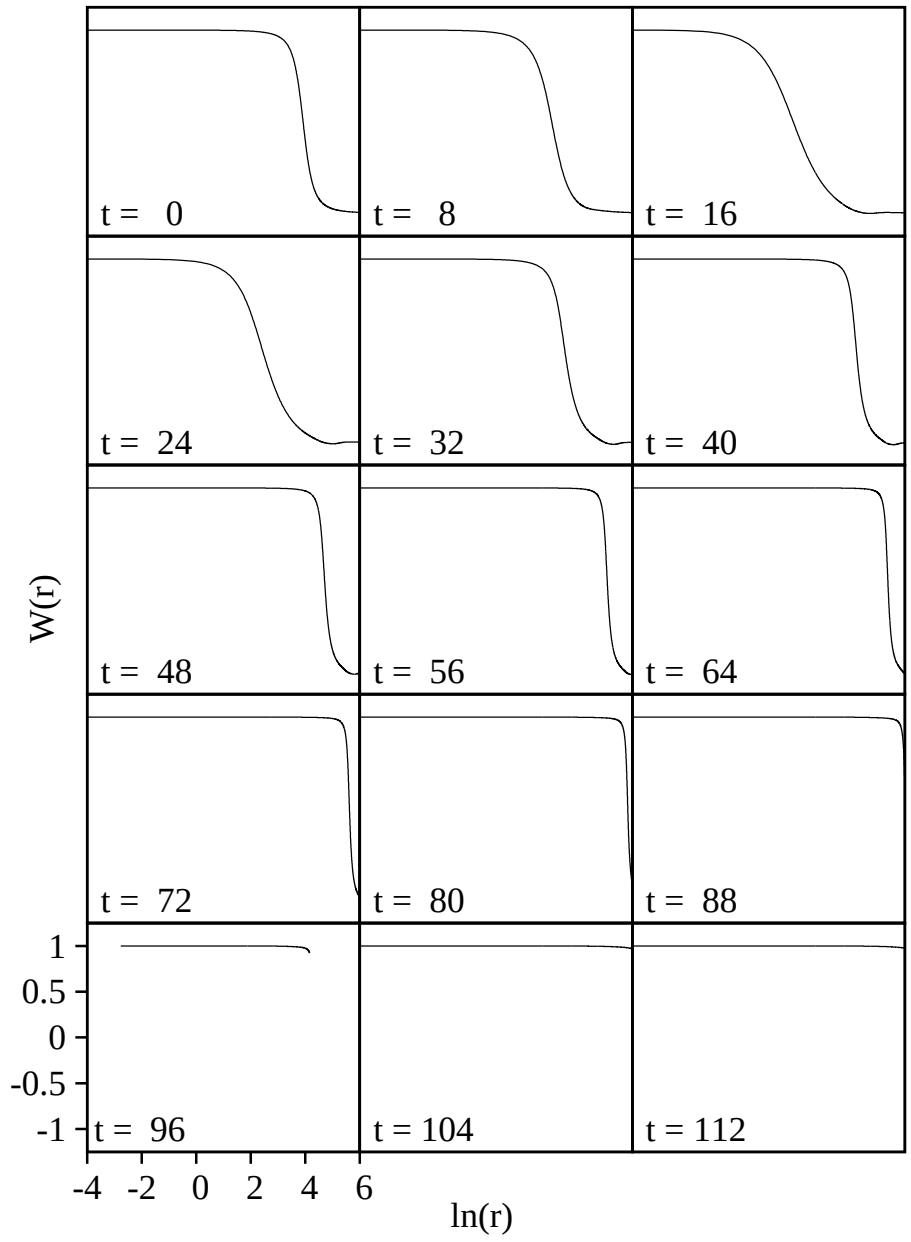


Figure 4.2: Evolution of the Yang-Mills field variable $W$ over time for the subcritical case. Initially the profile is ingoing, but at smaller radii scatters through the origin, eventually dispersing to infinity. Flat space is left behind as the final state of the system.

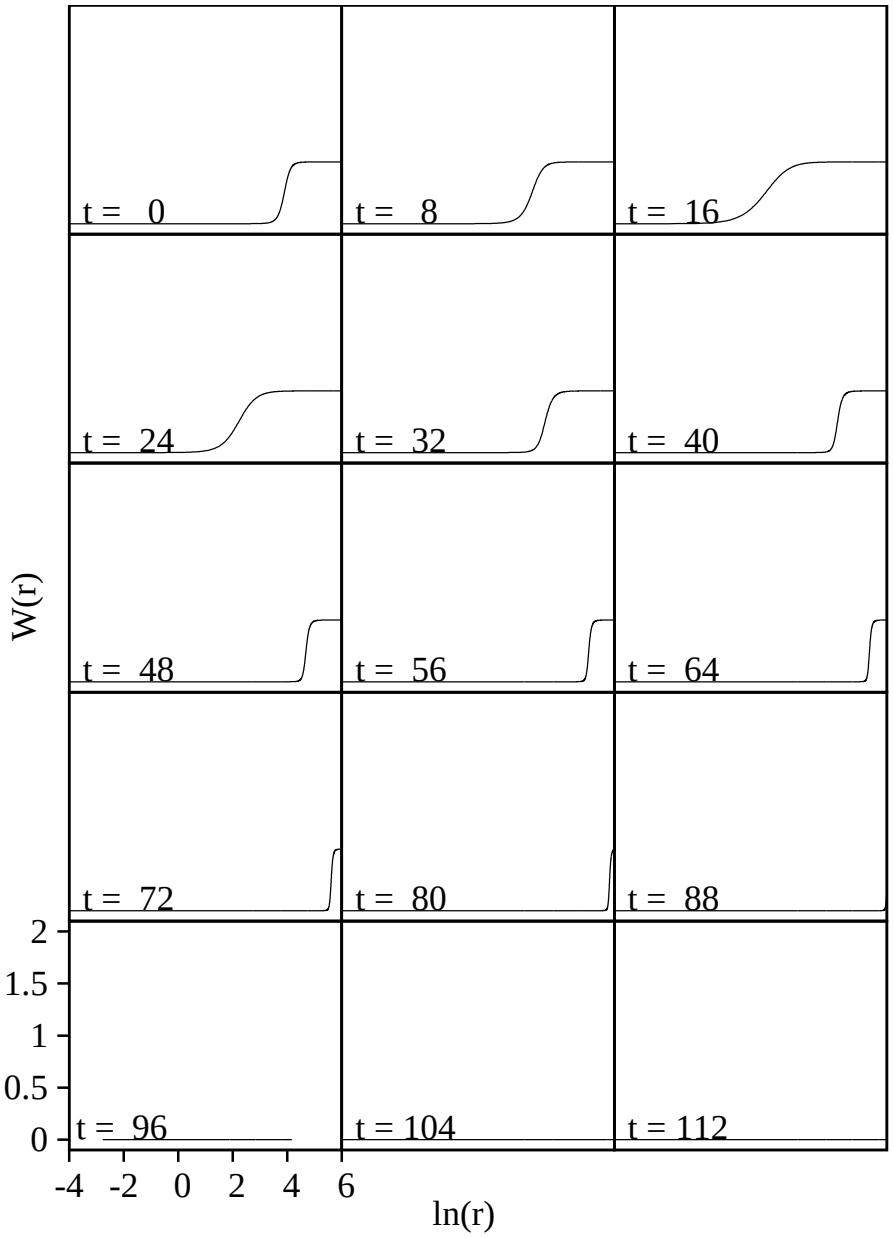


Figure 4.3: Evolution of the gravitating mass of the Yang-Mills field over time for the subcritical case. Initially the profile is ingoing, but at smaller radii scatters through the origin, eventually dispersing to infinity. Flat space is left behind as the final state of the system. Note that mass is conserved at the outer boundary until the field propagates off of the computational domain.

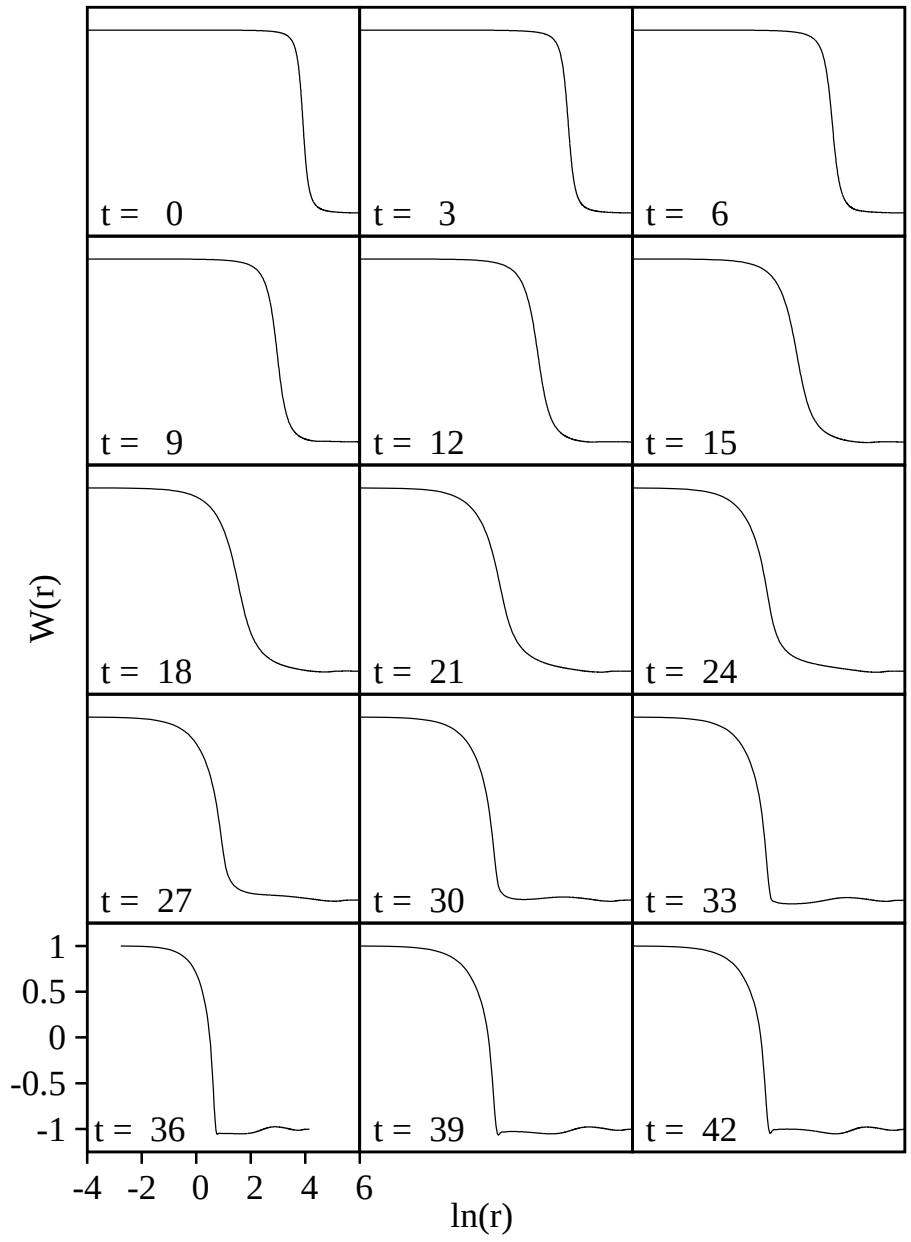


Figure 4.4: Evolution of the Yang-Mills field variable $W$ over time for the supercritical case. Note the irregularities appearing in the solution at later times; this is characteristic of the formation of a black hole in the chosen polar-areal coordinates.

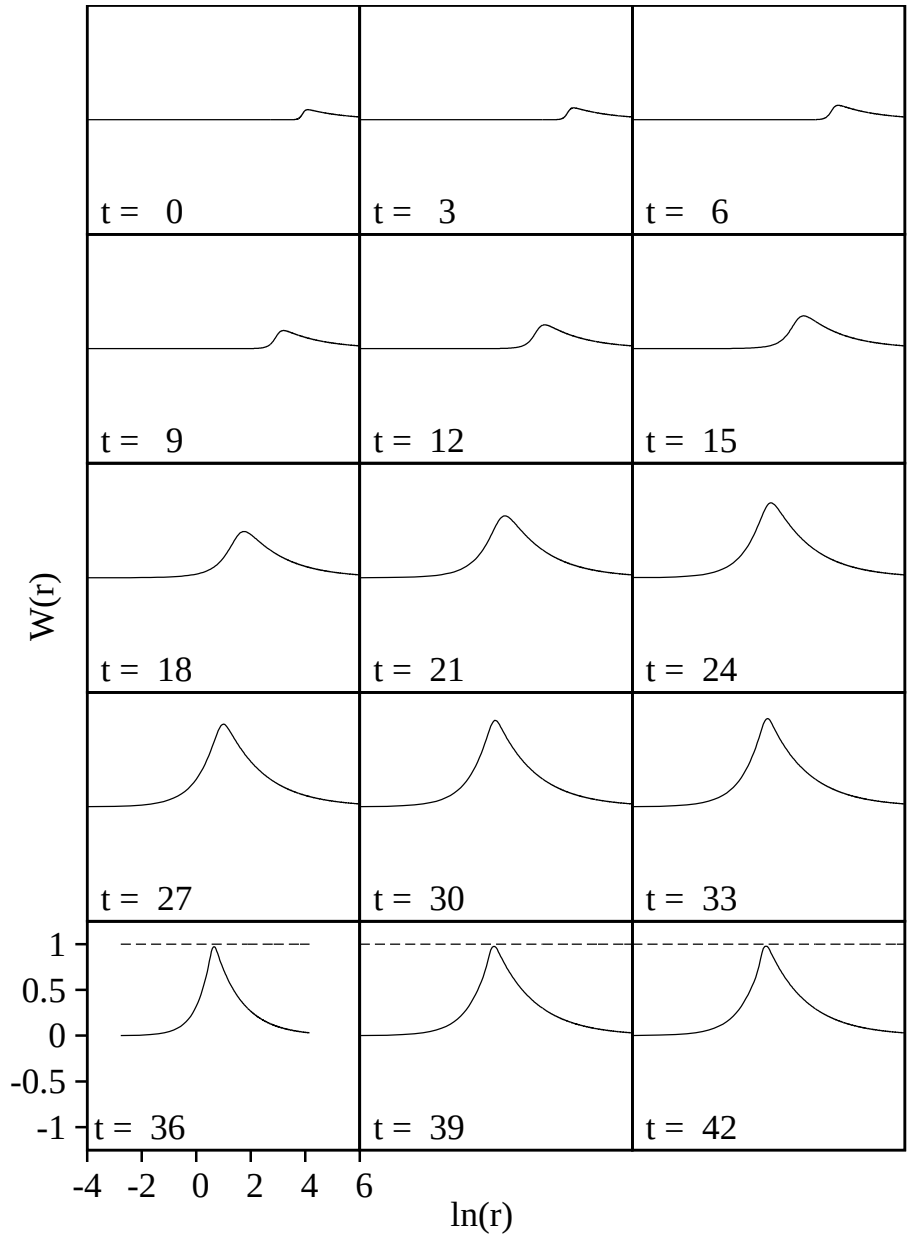


Figure 4.5: Evolution of the function $2m/r$ for the gravitating mass $m$ of the Yang-Mills field in the supercritical case. The rapid asymptote to 1 is indicative of black hole formation. This occurence at a finite radius shows the finite mass of the black hole created. As this solution is not close to the critical solution, this is to be expected.

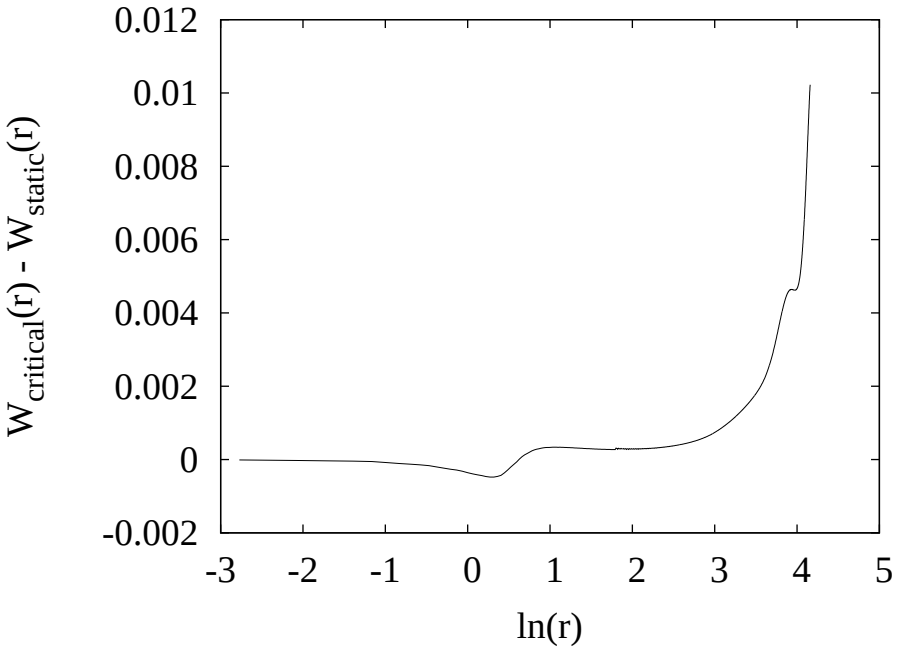


Figure 4.6: Comparison of $W$ for the near-critical case, with $|p - p^*|/p^* \approx 10^{-16}$, with the static solution discovered by Bartnik and McKinnon. The two agree best near the origin and increasingly differ at larger radii. This is likely caused by the fact that $W$ is derived by integrating $\Phi = W_t$ outwards from the origin in the first order method. The outer boundary condition is also likely to be responsible.

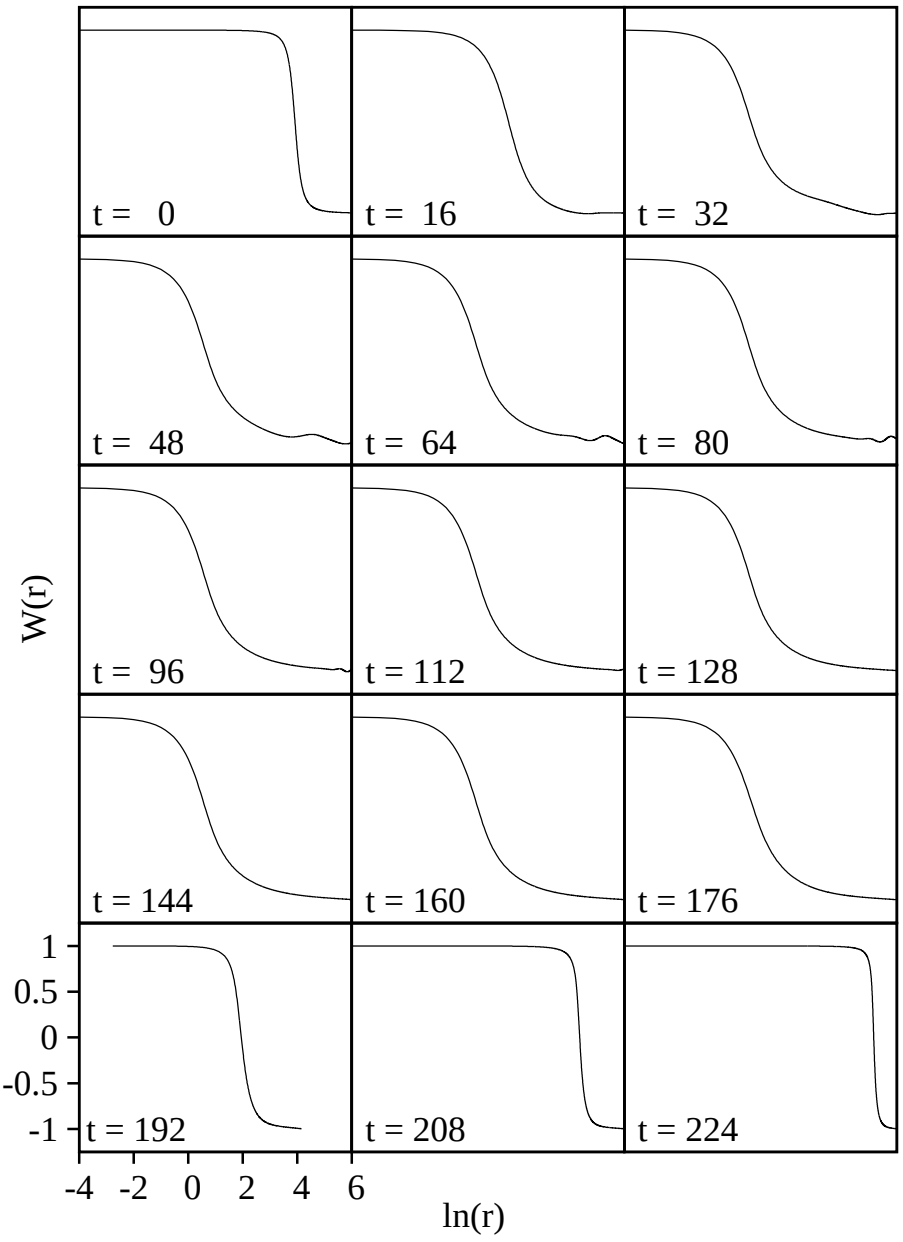


Figure 4.7: Evolution of the Yang-Mills field variable $W$ over time for the near-critical case, with $|p - p^*|/p^* \approx 10^{-16}$. Initially the profile is ingoing, but at intermediate times settles down at a nontrivial static solution. Eventually the field disperses to infinity due to lack of exact resolution for the critical value of the relevant initial data parameter.

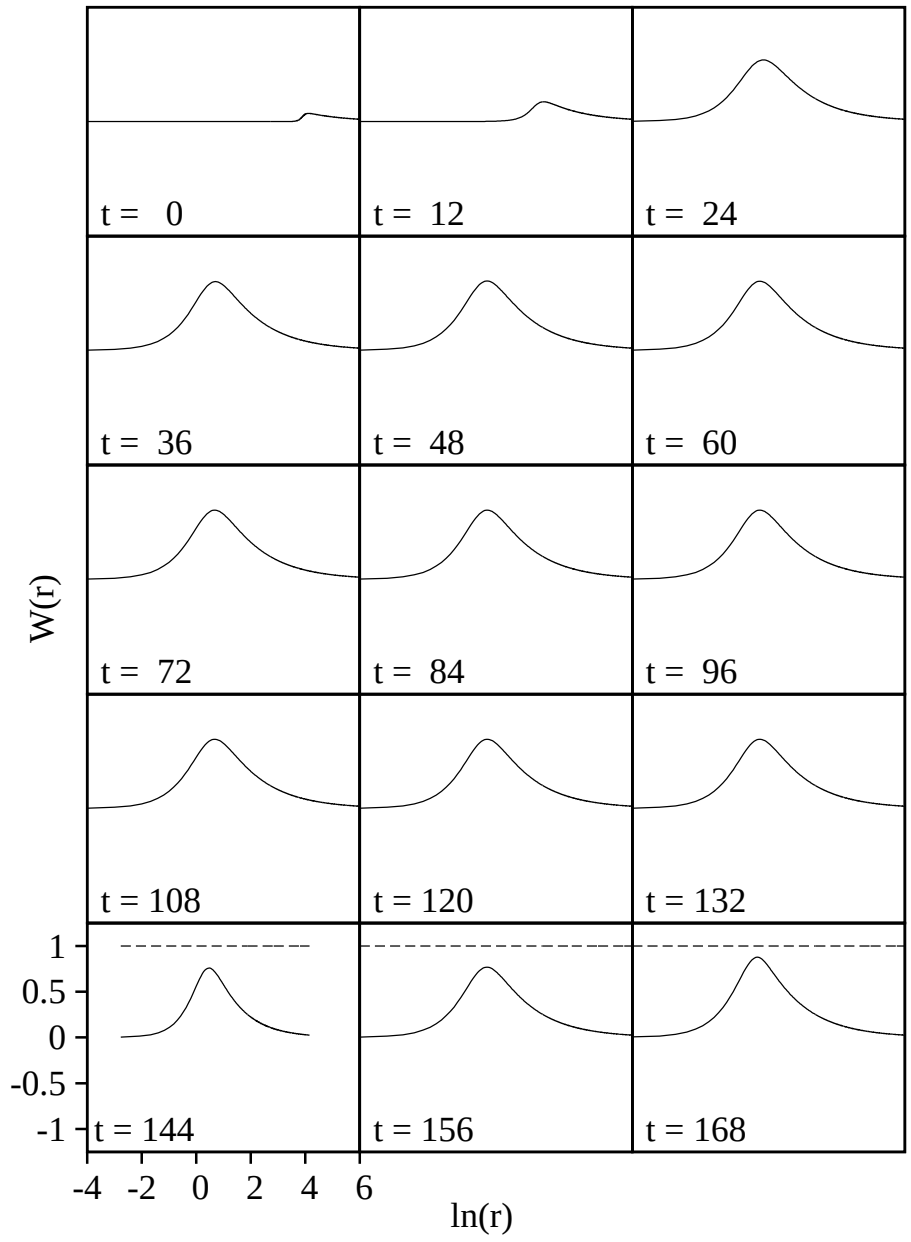


Figure 4.8: Evolution of the function $2m/r$ for the gravitating mass $m$ of the Yang-Mills field in the slightly supercritical case. The asymptote to 1 is indicative of black hole formation. This occurence at a finite radius shows the minimum mass of black hole created and the discontinuous change in the end state of the system as the initial data family parameter crosses its critical value.

that lifetime was instead measured in central proper time,

$$T \equiv \int_0^t \alpha(0,t')dt' \tag{4.2}$$

However, during the static phase of the evolution, $\alpha(0,t) = \alpha_o$ is constant. Thus $T = \alpha_o t$, so $T \sim \lambda \ln|p-p^*|$ means that $t \sim \ln|p-p^*|\lambda/a_o$. Thus $\lambda \approx \sigma\alpha_o$. Hence, with $\alpha_o = 0.126525$ for the first family of initial data, we obtain a value of $\lambda = 0.54949$. With $\alpha_o = 0.126526$ for the second family of initial data, we obtain a value of $\lambda = 0.52752$. The first is in good agreement with the previously determined value of $\lambda = 0.5520$. However, the value of $\lambda$ obtained for the second family of initial data deviates a small but significant amount; this could be due to a lack of resolution of the critical value of $r_o$, which could change $p-p^*$ enough to account for this discrepancy. All three of these $\lambda$ values are at least close, if off by a few percent from one another. This is a strong indication that the scaling exponent $\lambda$ truly is independent of the family of initial data chosen.

## 4.2 First Order Methods Convergence Testing

We need to ensure that the solution to the finite difference approximations is a good representation of the solution to the actual continuum problem. The first check of this is to ensure that the continuum solutions converge as the grid spacing $h \to 0$, and that they converge as quickly as expected. Since we are using $O(h^2)$ discretizations, the discrete solution should have $O(h^2)$ error. To confirm this, we check the quantity $C^h(x^\mu)$, as defined in (3.12), to compare the discrete solutions as the grid size decreases. Figure 4.10 shows the $L_2$ norm on the radial domain interval [0,$r_{\max} = 64$] of $C^h$ over time. At the smallest grid spacing there are $N = 8193$ grid points covering the spatial domain, resulting in a grid spacing of $h = 0.0078125$. Also a Courant number of $\lambda = 0.5$ was chosen. This shows that as the basic grid spacing $h_0 \to 0$, $C^h$ approaches $4 = 2^2$ for our $O(h^2)$ method. This quantity is closest to 4 until the ingoing pulse scatters off of itself and starts dispersing. At later times $C^h$ is higher, likely due to effects at the origin.

Convergence does not necessarily imply convergence to the solution of the continuum problem. Without knowing the continuum solution, this cannot be proven directly. However, we can be reasonably certain that the discrete solutions are converging to the correct solution by building up evidence that shows consistency between the actual convergence and what the correct convergence would look like.

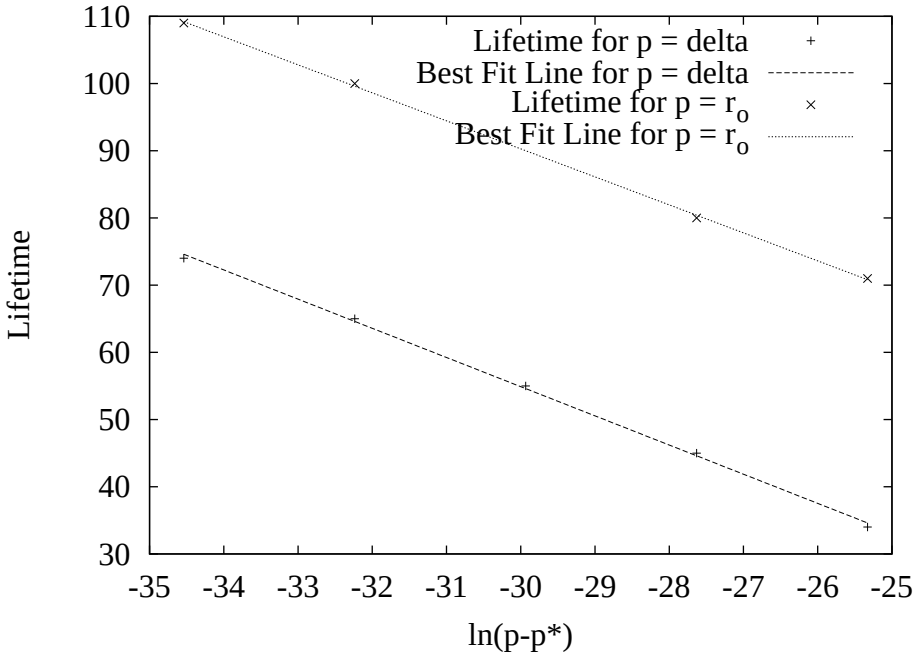


Figure 4.9: Lifetime of the critical 'kink' solution as a function of the initial data parameter $p$. The exponential dependence of the lifetime on the parameter difference $p - p^*$ is shown with the line of best fit. The slopes of the best-fit lines are nearly equal; this is an example of the universality of the scaling exponent across different families of initial data.

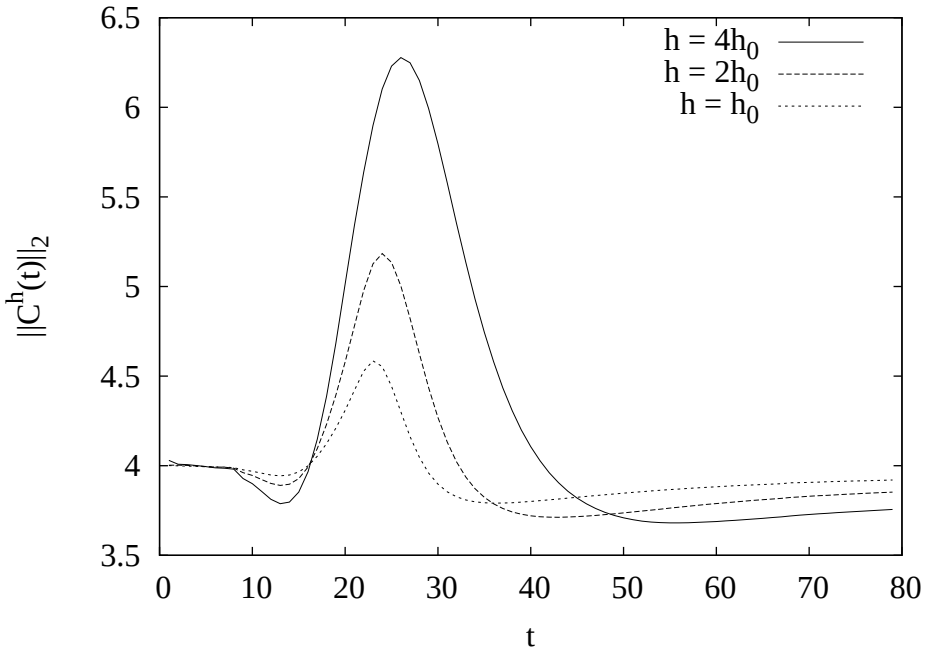


Figure 4.10: $L_2$ spatial norm of the convergence quantity $C^h$ as a function of time for several grid spacings. The minimum spacing is $h_0 = 0.0078125$. As the grid spacing $h$ decreases towards $h_0$, the convergence quantity approaches the value 4. Effects at the origin are the likely primary cause of the increase in $C^h$ over time, particularly for $10 \lesssim t \lesssim 50$.

The most accessible piece of evidence is rooted in the physics of the problem — conservation laws. If a finite difference approximation is implemented incorrectly, or if its solution somehow does not converge to the continuum problem, it is highly unlikely that these solutions would obey the physical conservation laws. For this problem, the total mass is conserved, and also is easily calculated, making mass conservation an excellent check for proper convergence. Figure 4.11 shows the mass at the outer boundary, for the case of the critical solution, as a function of time. These curves clearly show that although the computed total mass fluctuates as a function of time for any finite grid spacing $h$, the fluctuations become smaller as $h \to 0$, and indeed appear to be $O(h^2)$ as expected.

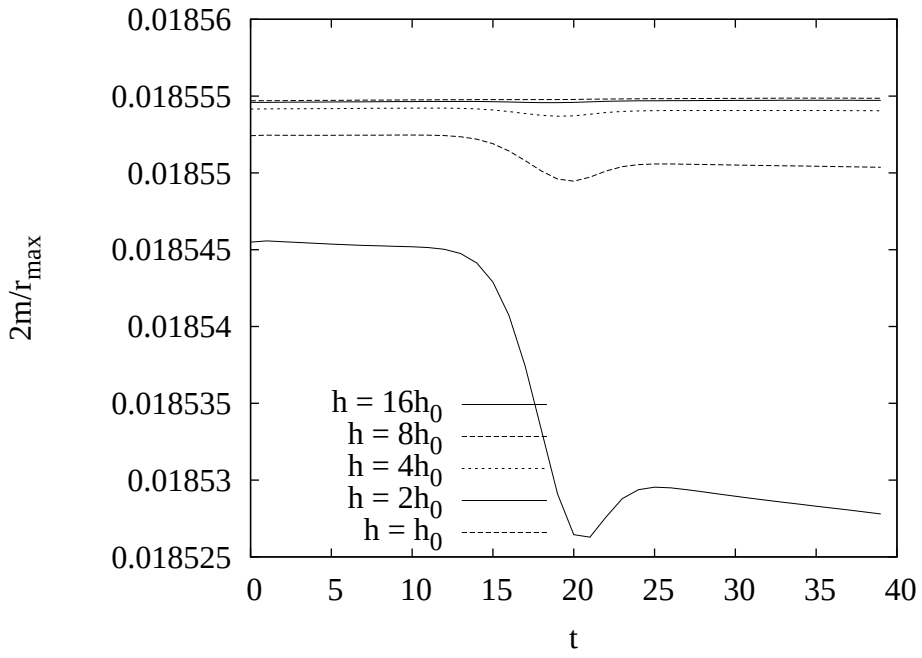


Figure 4.11: The function $2m/r_{\max}$ at the outer boundary. For the initially ingoing data the mass collapses inwards along with the field, resulting in a nearly constant mass at the outer boundary until the field disperses, along with the mass, off of the computational domain. As the grid spacing $h$ decreases, the outer boundary mass converges to a constant value for this initial period of time.

## 4.3 Second Order Methods

As discussed previously, second order methods provide a different discretization for the same problem. Although slightly more difficult to implement than first order methods, they are just as effective in giving the evolution for $W$. One way in which they do differ from the first order methods is in how we create approximately ingoing initial data, as detailed in §2.5.2.

This difference causes a change in the critical parameter values. With $r_o = 15$ as in the first order case, the critical value for the second order method is $\delta = 1.75285780266774$. Here, we have $N = 1029$ grid points covering the spatial domain [0,64], resulting in a grid spacing of $h = 0.062256809$. Also, a Courant number of $\lambda = 0.25$ was chosen.

The difference in initialization also causes qualitative changes in the behaviour of the solution as it collapses and disperses. However, it is an excellent way to illustrate the universality of the critical solution, which, to the level of numerical error, is the same for both methods. Figure 4.12 shows the evolution for the critical solutions for both first and second order methods. Note that both solutions settle down to the same static solution, though the initial data for the second order method causes additional wave-like behaviour in the solution at larger radii. Also, due to different resolutions obtained for the critical parameters, the second order method results in a near critical evolution whose lifetime is shorter than for the first order case.

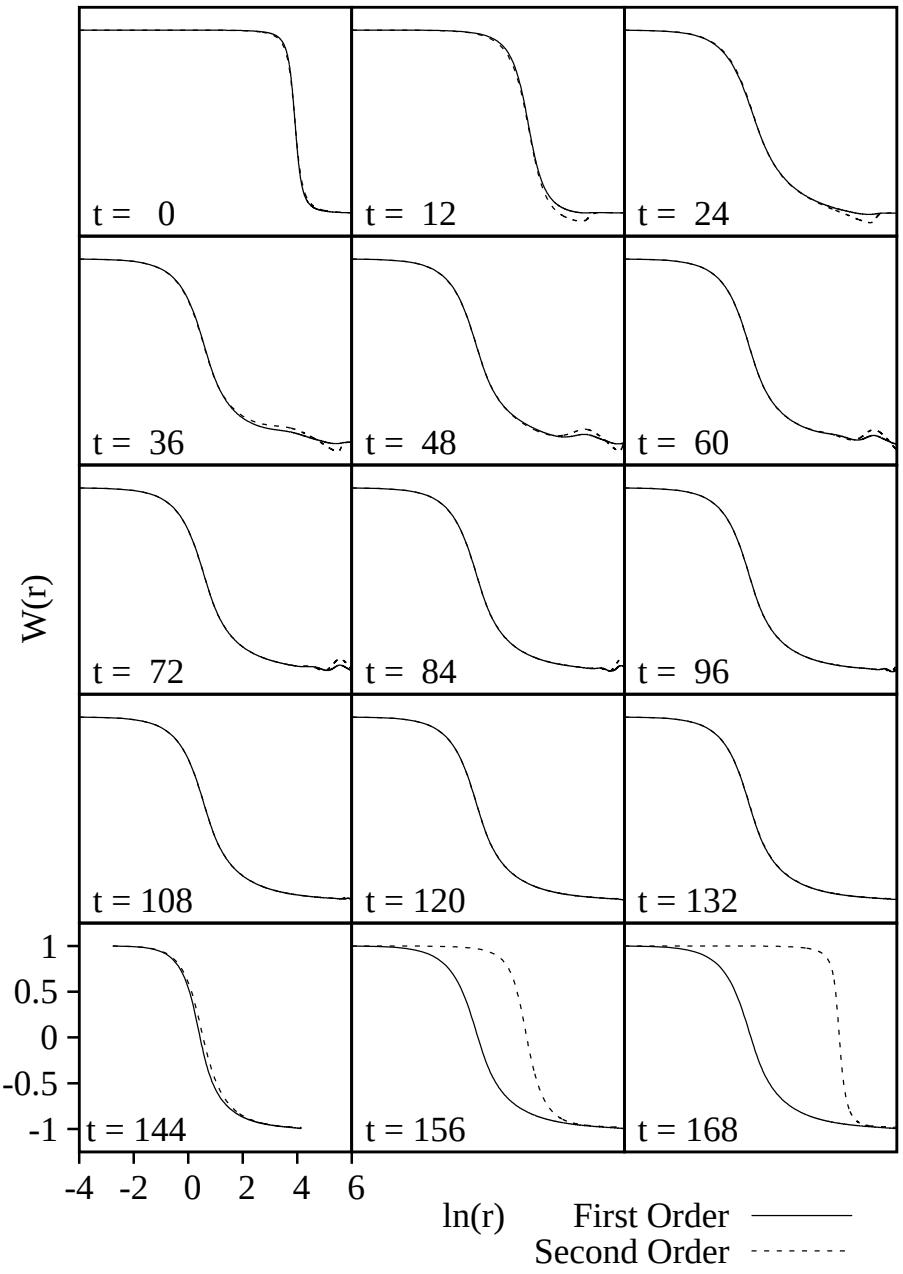


Figure 4.12: Evolution of the Yang-Mills field variable $W$ over time for the critical solution. Solutions for both the first order method and second order method are shown, each with different choices for ingoing initial data. While the detailed evolution is different in the two cases, both solutions settle down to the same static critical solution, showing its universality.

# Chapter 5

# Conclusion

We used the SU(2) Yang-Mills field as a representative of non-abelian gauge theories in order to study their dynamics when coupled to the gravitational field as described by the theory of general relativity. An abelian gauge, magnetic ansatz field was assumed, along with spherical symmetry, to simplify calculations. However, the behaviour of the field is still quite complex. We confirm the existence of type I critical behaviour for this field, finding minimum mass black hole formation, static critical solutions and scaling of near-critical solution lifetimes.

Finite difference approximations were used to solve the partial differential equations governing the model. Two different approaches to making these difference approximations are compared. One was the use of a first order in time method. Here, auxiliary variables were defined in such a way that the equations of motion reduced to a larger set of equations, each explicitly an equation for a time derivative of an auxiliary variable. The simplification this offers the equations, as well as the ease of creating a finite difference scheme for single derivatives, has made this the traditional choice for numerical work in relativity. Also, all time derivatives in the equations are given explicitly, easing the creation of a finite difference system that evolves the system in time. The other approach is to use second order in time method. In this method, no auxiliary variables are defined, and for the case considered it was necessary to discretize an equation with second derivatives, both spatial and temporal. Constructing the finite difference scheme is slightly more involved but not qualitatively more difficult. Working directly with the fundamental variables, this method obviates any potential issues arising from the derivation of the fundamental variables from the auxiliary ones.

The second order method compared quite favourably with the first order method. Program runtimes are comparable, as are the grid spacings needed to obtain a similar degree of accuracy. For a relatively simple system, such as the one considered in this investigation, the two methods do not seem to differ significantly, except that the first order method provides an easier system to discretize. Since derivation of fundamental variables from auxiliary ones in this case reduced to one-dimensional integration, it was likely not

a complicated enough process to introduce any error that cannot be controlled by making the grid spacing slightly smaller. However, unpublished calculations seem to imply the breakdown of the first order in time method when applied to certain systems, and the second order method has been successfully utilized in the full-dimensional non-symmetric case [15]. The success of second order methods in this simple case argue for its possible use in more general problems with SU(2) Yang-Mills fields. These problems would remove the restrictions imposed in this work, such as the magnetic ansatz and the imposition of spherical symmetry.

# Bibliography


[1] A. Abrahams and C. Evans. *Phys. Rev. Lett.*, 70:2980, 1993.

[2] R. Arnowitt, S. Deser, and C. Misner. The dynamics of general relativity. In L. Witten, editor, *Gravitation — an Introduction to Current Research*. Wiley, New York, 1962.

[3] J. Bardeen and T. Piran. *Physics Reports*, 96:205, 1983.

[4] R. Bartnik and J. McKinnon. *Phys. Rev. Lett.*, 61:141, 1988.

[5] M. Choptuik. *Phys. Rev. Lett.*, 70:9, 1993.

[6] M. Choptuik. PhD thesis, The University of British Columbia, 1986.

[7] M. Choptuik, T. Chmaj, and P. Bizon. *Phys. Rev. Lett.*, 77:424, 1996.

[8] M. Choptuik, E. Hirschmann, S. Liebling, and F. Pretorius. *Phys. Rev. D*, 68:044007, 2003.

[9] Matthew W. Choptuik, Eric W. Hirschmann, and Robert L. Marsa. *Phys. Rev.*, D60:124011, 1999.

[10] R. Courant, K. Friedrichs, and H. Lewy. *IBM Journal*, 11:215, 1967.

[11] C. Gundlach. *Physics Reports*, 376:339, 2003.

[12] Gordon Kane. *Modern Elementary Particle Physics*. Perseus Books, Reading, Mass., 1993.

[13] David Merritt and Milos Milosavljevic. Massive black hole binary evolution. *Living Reviews in Relativity*, 8(8), 2005.

[14] C. Misner, K. Thorne, and J. Wheeler. *Gravitation*. W.H. Freeman, San Francisco, 1973.

[15] Frans Pretorius. *Class. Quant. Grav.*, 23:S529–S552, 2006.